

SUBMERSIBLE INVESTIGATION OF AN EXTINCT HYDROTHERMAL SYSTEM ON THE GALAPAGOS RIDGE: SULFIDE MOUNDS, STOCKWORK ZONE, AND DIFFERENTIATED LAVAS

ROBERT W. EMBLEY

*National Oceanographic and Atmospheric Administration, Hatfield Marine Science Center, Newport,
Oregon 97365, U.S.A.*

IAN R. JONASSON

Geological Survey of Canada, 601 Booth St., Ottawa, Ontario K1A 0E8, Canada

MICHAEL R. PERFIT

Department of Geology, University of Florida, Gainesville, Florida 32611, U.S.A.

JAMES M. FRANKLIN

Geological Survey of Canada, 601 Booth St., Ottawa, Ontario K1A 0E8, Canada

MAURICE A. TIVEY

School of Oceanography, University of Washington, Seattle, Washington 98195, U.S.A.

ALEXANDER MALAHOFF

Department of Oceanography, University of Hawaii, Honolulu, Hawaii 96822, U.S.A.

MICHAEL F. SMITH

Department of Geology, University of Florida, Gainesville, Florida 32611, U.S.A.

TIMOTHY J.G. FRANCIS

Institute of Oceanographic Sciences, Wormley, Godalming, Surrey, England GV8 5UB

ABSTRACT

Fifteen dives along the Galapagos Ridge in the region between 85°49' W and 85°55' W were made to examine the detailed relationships among tectonics, hydrothermal activity and lava compositions. Extensive tectonic activity and physical weathering have exposed the inner parts of large Cu-Zn sulfide mounds and the uppermost part of the underlying stockwork zone. The mineralization occurs at the top and southern base of a horst block, 40 to 80 m high, that separates the present Neovolcanic Zone to the north from an older rift valley to the south. The lavas in the Neovolcanic Zone are homogeneous MORB pillows; those on the horst block and within the southern valley are evolved MORB to andesite pillow and sheet flows. The alteration zone exposed beneath the sulfide mounds comprises a network of fracture-controlled pipe and sheet-like bodies of highly altered material which changes outward into relatively fresh but similarly closely fractured rocks. The hydrothermal upflow zone is extensively brecciated on a centimeter scale and encloses a stockwork of veinlets now filled largely by silica, clays and sulfides. The most highly altered rocks are strongly depleted in Ca, Na, K and Mn, and are enriched in S, Fe, Cu and Zn relative to their fresh analogs. Si and Mg are variable, the latter showing local depletions and enrichments according to the proportion and distribution of chlorite. Depletions in ¹⁸O with increasing ⁸⁷Sr/⁸⁶Sr suggest extensive seawater-rock interaction (W/R up to 100:1) at T up to 350°C. Deep-tow and ALVIN-based magnetic profiles have a relative magnetization low centered over the southern valley and the horst block that

could reflect more extensive hydrothermal alteration zones associated with the older seafloor. The Galapagos stockwork is most analogous to the alteration zones associated with massive sulfide deposits in the ophiolites of Cyprus and Oman.

Keywords: Galapagos Ridge, spreading center, alteration pipe, sulfides, stockwork, copper, chlorite, smectite, andesite, basalt, magnetic profile, isotopes.

SOMMAIRE

Nous avons effectué quinze plongées le long de la crête des Galapagos, entre 85°49' W et 85°55' W, afin de déterminer les relations entre l'activité tectonique et hydrothermale et la composition des laves. Une activité tectonique et une dégradation physique importantes ont contribué à exposer les parties internes de vastes amonçlements de sulfures de Cu et de Zn, ainsi que d'une vallée de rift plus ancienne au sud. La zone néovolcanique contient des laves en coussins, homogènes, de type MORB; les laves en coussins et les coulées en feuilles affleurant sur le horst et dans la vallée du Sud correspondent à une composition variant entre celle d'un MORB évolué à celle d'une andésite. La zone d'altération en dessous des monticules de sulfures contient un réseau de roches fortement altérées, disposées le

long des fissures verticales et horizontales, en s'éloignant desquelles à leur périphérie, ces domaines d'altération font place à des roches relativement fraîches mais également traversées par de nombreuses fissures. La zone de flux hydrothermal est fortement bréchifiée à l'échelle centimétrique, et renferme un stockwork de fissures qu'occupent maintenant de la silice, des argiles et des sulfures. Les roches les plus fortement altérées sont nettement appauvries en Ca, Na, K et Mn, et enrichies en S, Fe, Cu et Zn par rapport aux roches non altérées. Les teneurs en Si et Mg sont variables; les variations en teneurs du Mg reflètent la proportion et la distribution de la chlorite. L'appauvrissement en ^{18}O avec l'augmentation du rapport $^{87}\text{Sr}/^{86}\text{Sr}$ témoigne d'une interaction importante entre roches et eau de mer à des températures atteignant 350°C , avec un rapport eau/roche pouvant atteindre 100:1. Les profils magnétiques obtenus par remorquage de magnétomètres à grande profondeur et à bord du sous-marin ALVIN révèlent une région à faible champ magnétique centrée sur la vallée du Sud et sur le horst: elle pourrait indiquer l'existence de zones d'altération hydrothermale plus étendues, impliquant le socle. Le stockwerk de la crête des Galapagos ressemble fortement aux zones d'altération associées aux gisements de sulfures massifs de Chypre et d'Oman.

Mots-clés: crête des Galapagos, centre de séparation des plaques, altération d'un conduit, sulfures, stockwerk, cuivre, chlorite, smectite, andésite, basalte, profil magnétique, isotopes.

INTRODUCTION

Since the discovery of active submarine hydrothermal vent systems in the late 1970s (Corliss *et al.* 1979, Rise Project Group 1980), comparisons have been made with orebodies exposed in ophiolite sequences (*e.g.*, Oman, Cyprus and Newfoundland) or Precambrian Shield areas (Franklin *et al.* 1981). An important feature of ancient deposits is the relative accessibility to the deeper sections of the hydrothermal system (either through outcrops or drilling). However, the "stockwork" or feeder zones that comprise the hydrothermal upflow regions beneath such sulfide bodies have been overprinted to variable degrees by later metamorphism and deformation that obliterated original mineral assemblages and textures. This complicates interpretations of chemical data, which must necessarily be based on mineralogical and textural observations.

In modern oceans the upwelling portion of the hydrothermal system is rarely exposed. Detailed studies of altered lava samples come from dredged samples taken in the Atlantic (Mottl 1983, Bonatti *et al.* 1976, Humphris & Thompson 1978, Delaney *et al.* 1987); these samples have provided a data base used widely in discussions of hydrothermal plumbing systems. However, the inherent inaccuracy in dredging, and the tectonic complexity of the Mid-Atlantic Ridge, make it difficult to place their samples in context within a "typical" hydrothermal system.

Delaney *et al.* (1987) described quartz-cemented sulfide-bearing breccias recovered in dredges and by submersible from near the Kane Fracture Zone. Renard *et al.* (1985) described veined stockwork-like samples from a scarp on the East Pacific Rise (EPR) at $18^\circ30'\text{S}$, but their bulk chemical data indicate minimal alteration relative to the Galapagos samples. Similarly, Bäcker *et al.* (1985) reported "mineralized basalt breccia and basalt with disseminated pyrite" from dredges on the EPR at 21.5°S , but no analyses were given.

Deep Sea Drilling Project Hole 504B on the flank of the Costa Rica Rift provides a "reference section" through oceanic crust that has undergone axial and off-axial phases of hydrothermal alteration (Alt *et al.* 1986). A zone of stockwork-like alteration occurs at 635–653 m. Although the stockwork zone presumably formed when the site was above the axial magma chamber (5.9 Ma), the exact timing and depth below the seafloor, and its relationship to any massive sulfide deposit is unclear.

In 1980 and 1981, several ALVIN dives along the eastern Galapagos (Cocos-Nazca) Spreading Center (Fig. 1) discovered and sampled an extensive massive sulfide deposit that formed from an extinct hydrothermal system (Malahoff *et al.* 1983). Both syn-depositional and post-depositional faulting had occurred in the mineralized zone; initial observations suggested the likelihood of underlying stockwork zones exposed along the normal fault systems. In 1985, an ALVIN dive series was conducted in this area to search for such stockwork zones. This report describes the geological setting and the physical and chemical nature of a fossil hydrothermal system that was discovered directly beneath the Galapagos sulfide deposits. This is the first discovery of a seafloor sulfide deposit that has a well-exposed contiguous "stringer zone".

GEOLOGICAL SETTING

The study area is centered at $0^\circ45'\text{N}$, $85^\circ50.5'\text{W}$ at a water depth of 2540 m along the south side of the main Galapagos rift valley (Figs. 1, 2). The active Galapagos vents (Corliss *et al.* 1979) are 20 to 30 km west, between $86^\circ01'\text{W}$ and $86^\circ14'\text{W}$. Water emanating from the latter vents at up to 17°C supports diverse suites of live animal communities (Corliss *et al.* 1979). No massive sulfides have been sampled in this area, although they have been noted in camera surveys (Ballard *et al.* 1982).

The recent structural evolution of this part of the Galapagos Rift probably has been complex. For instance, the presence of curved ridges and sharp along-strike discontinuities and topography (*e.g.*, southern valley), particularly south of the axis (Fig. 2), may mark the position of old DEVALs (Langmuir *et al.* 1986) or overlapping spreading centers that have been partly bypassed by late mag-

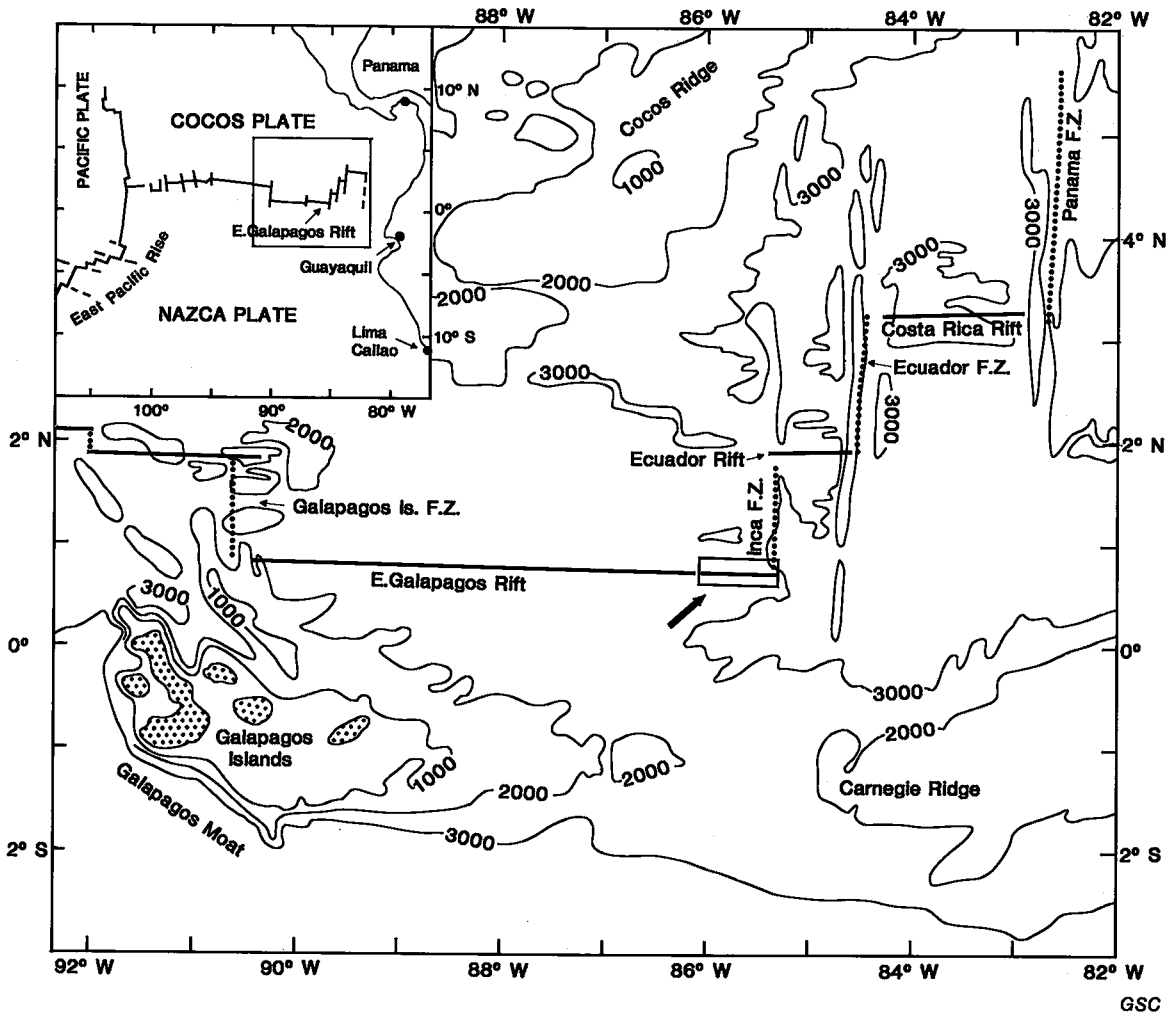


FIG. 1. Location of study area. Bathymetric contours in thousands of meters. Solid lines mark axes of spreading centers; dotted lines mark fracture zones. Location of Figure 2 shown by rectangular box near intersection of Eastern Galapagos Rift and Inca Fracture Zone.

matic events and rafted off-axis (Macdonald *et al.* 1984, 1986). The morphology of the Galapagos Spreading Center in the vicinity of the study area is unusual in that there appears to be a "double rift" structure.

The northern 1.5 km-wide rift valley is separated from the 1 km-wide southern depression by a narrow (30–60 m relief) ridge (Figs. 2 to 5). The north-facing scarp of the central ridge is on line with a projection of the main southern boundary fault of the Galapagos Neovolcanic Zone between $85^{\circ}58'W$ and $86^{\circ}12'W$, where many warm vents are located (Ballard *et al.* 1982). A band of young, glassy pillow flows a few hundred meters north of the ridge

marks the trace of the Neovolcanic Zone through this part of the Galapagos Spreading Center. Cores taken in the southern valley contain up to 40 cm of pelagic sediment, indicating up to 15 thousands of years of sedimentation on the lava fields (Lalou *et al.* 1983). At least 10 cm of sediment also cover pillow lavas and oxidized sulfide mounds on top of the ridge. The sparsely sedimented lavas within the central part of the northern rift valley (Neovolcanic Zone) are apparently younger.

Most of the ALVIN dives were made in a small area (2×1 km) centered at $0^{\circ}45'N$, $85^{\circ}50.5'W$, where major sulfide mounds were sampled during reconnaissance dives in 1981. The bathymetry shown

in Figure 4 was derived from pressure–depth readings from ALVIN. The horst on the map shoals to a narrow, flat top that is only about 100 m wide in the vicinity of the sulfide mounds. The discrepancy between the minimum depth on the Sea Beam bathymetric map (Fig. 3) at about 2590 m, *versus* the ALVIN-based map (about 2535 m) is largely a result of the resolution of the Sea Beam system; *i.e.*, the width of the top of the horst is less than the “footprint” (120 m) of the Sea Beam system at this depth. In addition to a relatively dense grid of mapping and sampling conducted within the area on Figure 4, there were also lava sampling excursions to the north and south within the Neovolcanic zones and in an area of andesite flows, respectively. In particular, dive 1652 traversed the entire rift valley from north to south (Fig. 3). Another area of sulfides, and an area of silica–manganese dioxide mounds emanating warm water ($\sim 10^\circ\text{C}$) are located about 5 km to the west ($85^\circ 54' \text{W}$, Fig. 2); these also were sampled (dives 1660, 1661, and 1663). All mineralization seems to have formed along an extension of the same geologic boundary that occurs within the primary study area. We interpret the central ridge as a fault-bounded horst on the basis of pervasive talus slopes, vertical walls of truncated pillows, and the presence of truncated sulfide mounds on the top and also at the base of the southern scarp.

LAVA PETROLOGY, GEOCHEMISTRY AND SPATIAL MORPHOLOGY

The 1980/81 dive series recovered a diverse suite of evolved N-type mid-ocean ridge (MOR) tholeiitic lavas, including FeTi basalt and andesite from an area along the ridge within 60 km of the Galapagos Rift – Inca Transform intersection (Fornari *et al.* 1983, Perfit *et al.* 1983). Some of the most chemically evolved lavas were sampled near the sulfide deposits (Malahoff *et al.* 1983). Within the Neovolcanic Zone, from the study area to about $86^\circ 13' \text{W}$, the rocks are significantly less differentiated; FeTi basalt is rare and andesite absent (Fornari *et al.* 1983, Ballard *et al.* 1979). On the basis of petrological and geochemical data, Perfit *et al.* (1983) proposed that extensive crystal–liquid fractionation occurred at shallow levels in isolated magma chambers (approximately 2 km depth) in response to increased thermal budgets during attempted ridge propagation close to the Galapagos Rift–Inca Transform inter-

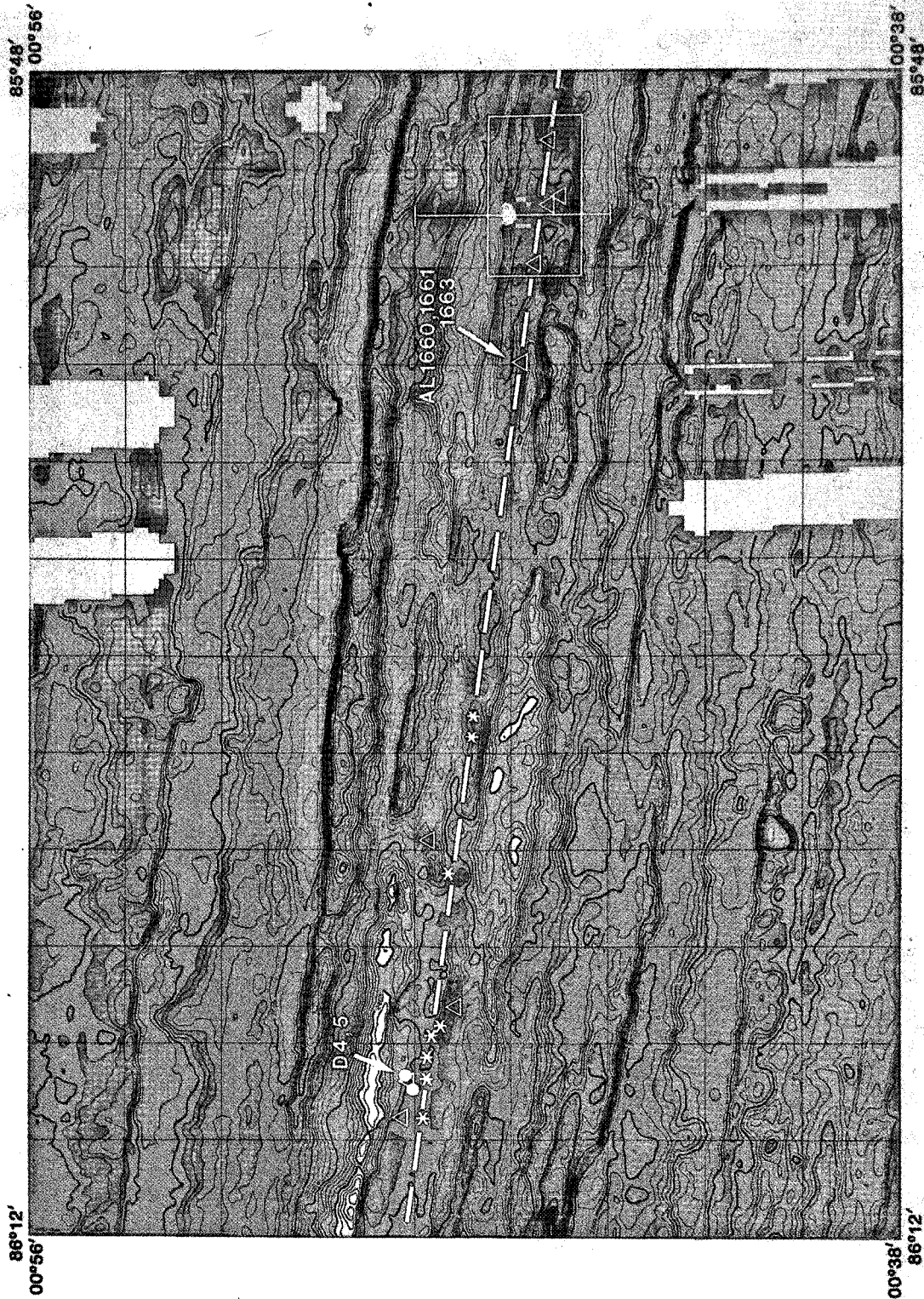
section (Fig. 1). They also proposed that massive sulfide generation in this region might have been enhanced by increased concentration of sulfides in highly evolved lavas, and their subsequent remobilization during hydrothermal circulation.

Extensive sampling near the sulfide mounds during the 1985 series of dives, together with subsequent geochemical investigations, have allowed us to place further constraints on the spatial association between these sulfide deposits and highly fractionated MOR magmas. The predominant rock type recovered in 9 dives (1647–1655, Table 1) that traversed the southern rift valley and central horst area was FeTi basalt ($\text{FeO}_T > 12 \text{ wt.}\%$, $\text{TiO}_2 > 2 \text{ wt.}\%$), and some of these are highly evolved ($\text{FeO}_T > 16 \text{ wt.}\%$, $\text{TiO}_2 > 3 \text{ wt.}\%$). In addition, basaltic andesite and andesite (SiO_2 54–60 wt.%) are abundant within the southern valley and are very common along the central horst (Fig. 4). Chemical analyses of representative rock types are given in Table 1; the FeTi basalt and andesite recovered from this limited area have chemical compositions that closely match those determined in previous studies (Fornari *et al.* 1983, Perfit *et al.* 1983). Typical mafic MORB was rarely recovered in the southern rift valley and around the horst near sulfide mounds (Figs. 4, 5). However, MORB was recovered a few hundred meters west of the alteration zone (Fig. 4; samples 1650–1, 1649–5). The dichotomy of rock types between the northern rift valley (Ballard *et al.* 1979), and horst/southern rift valleys is evident if indices of fractionation such as Mg-number are compared (Fig. 6).

Voluminous lobate flows of andesitic basalt and andesite occur near sulfide mounds in the southern rift valley and along the top and scarps of the horst. Some of these flows have a characteristic blocky appearance and lack the surface decoration (*i.e.*, surface corrugations or protuberances) common to basaltic pillow lavas. The andesite is slightly vesicular, extremely glassy, has conchoidal fracture, and ranges from dark brown to green to bluish grey.

FeTi basalt was the most common lava type sampled and was recovered with andesite at a few localities. It occurs as small pillows with thin glass crusts or as slightly vesicular sheet flows ($< 4 \text{ cm}$ thick). On the horst top (1651–4) FeTi basalt forms small, irregular-shaped spires (about 1 m high) similar to “dribble spires” elsewhere found associated with subaerial “aa” flows.

FIG. 2. Multibeam bathymetric chart of axis of Galapagos Ridge in vicinity of study area. Combination of SASS bathymetry collected in 1976 by *U.S.N.S. Dutton* and Sea Beam collected in 1985 by *Atlantis II*. Contour interval is 20 m and color interval is 40 m. A continuation of the best fit line through the warm-water vents (dashed line) east of $86^\circ 00' \text{W}$ corresponds approximately to fault controlling locations of older sulfide mineralization and the southern part of the Neovolcanic Zone. Stars (*) indicate warm-water vents (Ballard *et al.* 1982); triangles locate massive sulfide mounds (this study and H. Bäcker, pers. comm.). D4, D5 refer to dredge hauls; AL1660, 1661, 1663 refer to ALVIN dives discussed in text. The box shows location of Figure 3; N–S line traces deep-tow magnetometer line (Fig. 11).



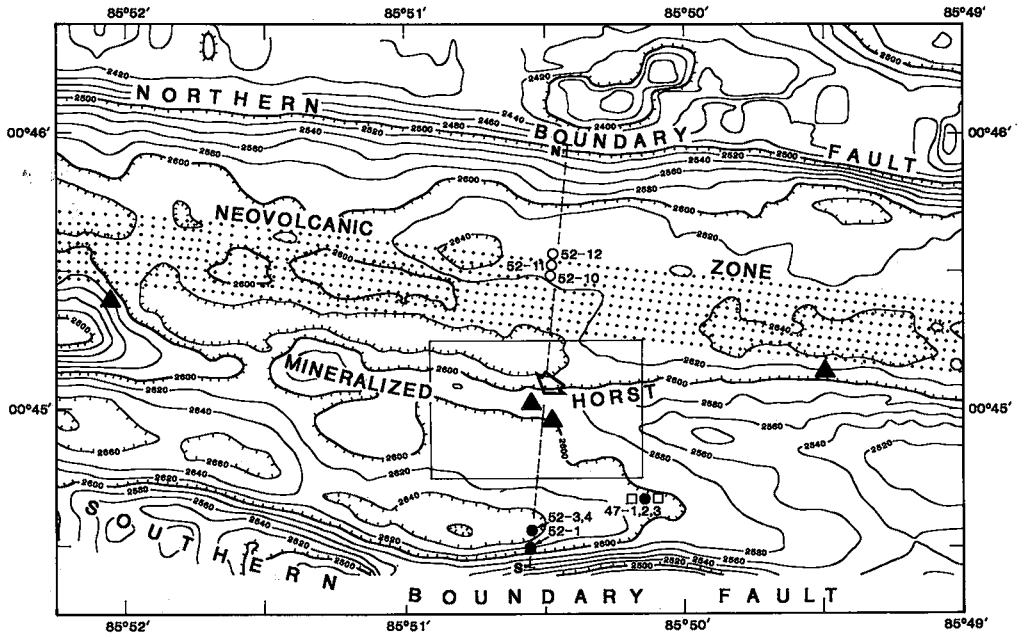


FIG. 3. Sea Beam bathymetry of Galapagos Rift in vicinity of study area. The triangles show locations of largest massive sulfide mounds; the arrow indicates the stockwork-zone outcrop. Neovolcanic Zone shown by stippling. Dashed line gives location of cross-section shown in Figure 5. Box is area of Figure 4. Sample designation same as Figure 5.

Lavas from the Neovolcanic Zone within the northern valley (Figs. 3, 5), in contrast with those to the south, are mainly moderately fractionated MORB or ferrobasalt (Table 1). The lavas typically form bulbous pillows with numerous small buds protruding from corrugated surfaces that are glassy and only lightly dusted with sediment. FeTi basalt and andesite have not been identified in the Neovolcanic Zone in this section of the Galapagos Rift (Fig. 5). However, some moderately evolved FeTi basalt was recovered from the medial rift zone during the 1980 dives. Notably, lavas recovered around the active vents at $86^{\circ}06'$ to $11'W$ (thermal springs of Corliss *et al.* 1979) are significantly less evolved and are more mafic than those associated with the inactive vent sites in the study area. Pillow and sheet-flow MORB samples (Ballard *et al.* 1979) contain 1.33 to 2.67 wt. % TiO_2 and have Mg-numbers of about 53 (Fig. 6). Earlier work indicated that lavas erupted along the Galapagos Rift within 60 km of the Inca Transform fault are more fractionated and chemically less homogeneous than those farther from the fault (Perfit *et al.* 1983). The results of the 1985 dive program support the earlier observation that the most recent period of volcanism along the Galapagos Spreading Center is associated both with less evolved lavas and, apparently, with little sulfide formation. Hydrothermal activity associated with the Neovolcanic Zone has generated a series of clay-silica

deposits around warm springs (Fig. 2; dives 1660, 1663).

SULFIDE DEPOSITS

In the study area the sulfide deposits occur as single chimneys and composite mounds scattered over an area of 0.5 km by 0.5 km (Figs. 3, 4), both in the southern valley and on top of the horst block. Mounds and chimneys are most extensive at the southern base of the horst block at a water depth of 2570–2580 m, where the horst block widens to the east into a series of fault-sliced blocks (Figs. 3, 4). The sulfides in the southern valley (1649 mounds) are in two morphologic settings: (1) individual chimneys and small mounds along the base of the main south-facing scarp of the horst block, and (2) large composite mounds of coalesced and collapsed chimneys, exceeding 100 m in diameter and about 10 m high, that occur along subsidiary parallel faults south of the primary fault (Fig. 7a). Most of the mounds are clearly associated with faults, but some large accumulations of sulfides may be covering underlying faults. Although most of the faults in this area are east-west trending, at least one sulfide mound with a north-south trend seems to be fault-controlled, suggesting the possibility of mineralized cross-structures. In several places, small chimneys project out of the talus slope and drape against the main south scarp. As it is unlikely that such chim-

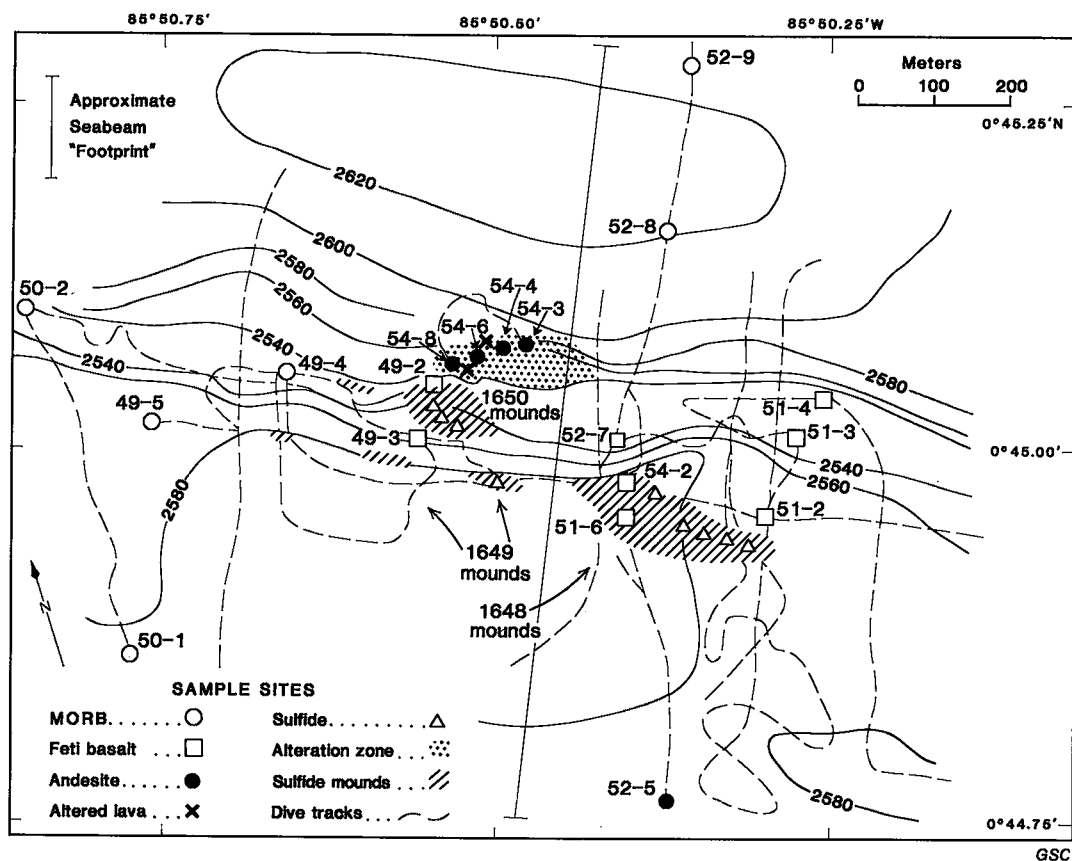


FIG. 4. Detailed bathymetry of dive area showing dive tracks, location of samples (e.g., 54-4 designates Dive 1654, station 4), and lava types. Samples 1654-6, 7, 8 all are from the same site; 1655-1 not located for space reasons. Samples on wall projected to 2537 m (horst top). Box on Figure 3 shows area covered on map. Depths (m) based on ALVIN pressure gauge. N-S line indicates position of cross-section in Figure 5.

neys could survive rock falls, this observation strongly implies some post-tectonic mineralization.

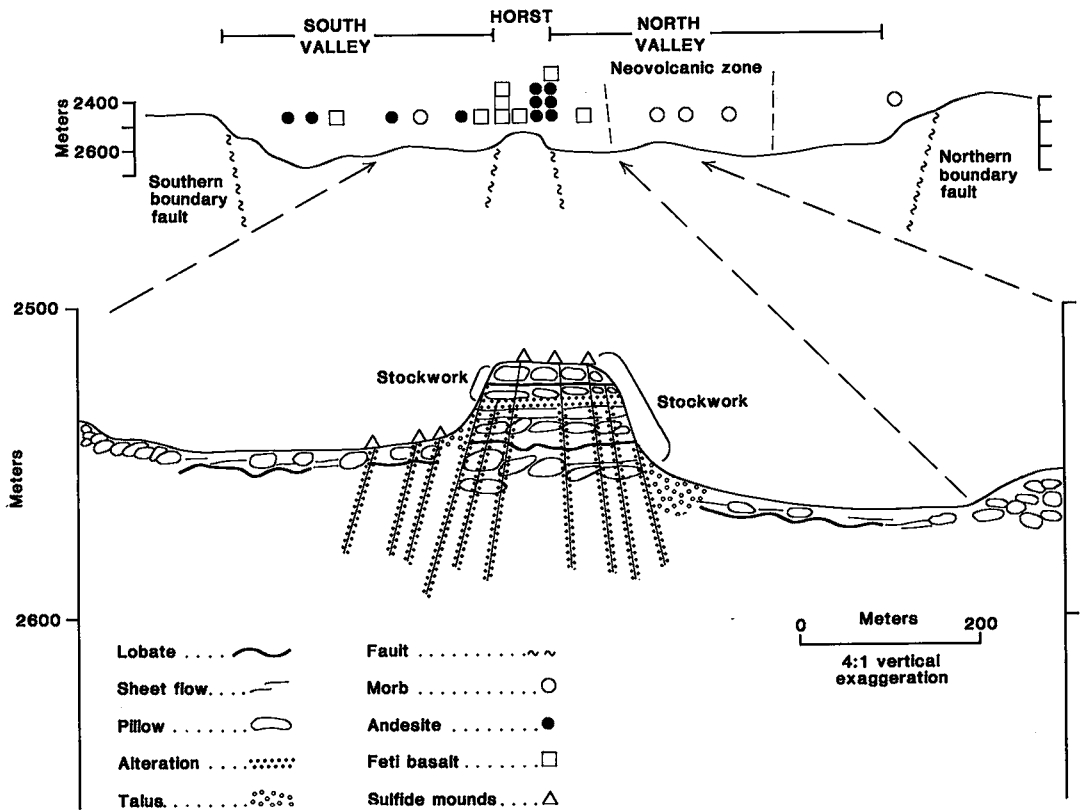
A nest of sulfide mounds and chimneys on top of the horst at a depth of 2535 m was also sampled (Fig. 4; 1650 mounds). These deposits are heavily sedimented, are scattered over an area of about 100 m in diameter, and also appear to be associated with east-west faulting. Some mounds are truncated by the north scarp that exposes underlying altered lavas (Fig. 7b).

The unweathered sulfides consist principally of pyrite and chalcopyrite with minor sphalerite, pyrrhotite and marcasite. From the areal extent and exposed thickness of sulfides observed, the total amount of sulfide is 1.5 m tonnes in the study area (Fig. 4). The high ratio of Cu to Zn (about 6:1) distinguishes the Galapagos sulfides from all other submarine deposits (Rona 1984, Malahoff *et al.* 1983, Kappel & Franklin 1988). Unweathered sulfides on top of the horst are compositionally indistinguishable

from most of those on the adjacent downthrown block (Table 2), suggesting that all the mound deposits in the area were formed under similar hydrothermal conditions.

Local oxidation and mass wasting of sulfides is common, both around mounds and within the primary talus slopes. Disintegrating chimneys are strongly depleted in all sulfides but contain silica (as quartz or amorphous silica), goethite, hematite, magnetite, and secondary copper minerals which include covellite, digenite, roxbyite, atacamite, botallackite and the Fe sulfate, szomolnokite. Rare barite rosettes and axiolites are enclosed in, or partly replaced by amorphous silica and pyrite in the margins of disintegrating chimneys.

Some ochrous mounds are composed mainly of siliceous iron oxide crusts and ferruginous mud. These represent the remains of wholly oxidized exteriors of chimneys and sulfide interiors, respectively. Areas where unweathered sulfides are exposed



GSC

FIG. 5. Top: generalized cross-section of Galapagos Rift through the study area showing location of features discussed in text. Lava samples have been projected onto cross-section (see Fig. 4 locations). Bottom: expanded cross-section through horst structure.

probably represent cores of composite stacks now exposed by mass wasting or exfoliation (e.g., Fig. 7a). The massive sulfides that survived prolonged supergene alteration have interiors that are richer in chalcopyrite and pyrite than in their outer walls. The latter consist of assemblages of pyrite-chalcopyrite-sphalerite-pyrrhotite.

ALTERATION AND STOCKWORK MINERALIZATION

An extensive outcrop of altered lavas from the uppermost section of a zone of primary hydrothermal upflow occurs on the north wall of the horst (Figs. 3, 4). Small outcrops were also observed high on the south-facing wall. The outcrop on the north wall extends 100 m laterally and 35–45 m vertically down to the talus pile at the foot of the wall. Volcanic rocks on the north wall consist of layers of glassy pillow lavas (predominantly basaltic andesite and andesite) interbedded with lobate and sheet flows (FeTi to ferrobasalt), and ponds of hyaloclastite

(andesite). The most accessible exposures lie within 10 to 15 m of the top of the horst (Figs. 7b to 7h); lower portions are partly obscured by talus and sediment. Alteration is pervasive and brecciation is extensive; however, pillow lobes, their selvages, and beds of glass shards generally are well-preserved as pseudomorphs and were easily mapped (Figs. 7f,g). Alteration is most pervasive in the hyaloclastite lenses because of their original high permeability. Mass wastage has differentially removed softer material from the horst and has given rise to a spectacular local topography of spurs, hoodoos, and overhangs that protrude from the face of the main escarpment (Fig. 7c). The amount of mass wastage depends on the nature of the parent volcanic rocks, the extent of brecciation, and the intensity of chemical alteration.

The innermost part of the alteration zone (Fig. 8) is typically light grey to white. Mud-free areas consist of smooth-faced slopes of soft, highly altered material and narrower patches of less altered, shat-

Table 1: Representative samples of fresh and altered lavas from the Eastern Galapagos Rift Southern Rift Valley

Locality		Northern Rift Valley including Neovolcanic Zone				Southern Rift Valley				Horst, Walls and Top around Alteration Zone										
Sample No. DAVE/ATH.	Type	52-9	52-10	52-12	59-1*	63-5	49-5**	50-2	51-2	52-3	52-4	52-5	52-5 ^o	47-1A	49-3	51-4 ^o	54-2	54-3A	54-4 ^o	54-6B
		bslt-p	bslt-p	bslt-p	bslt-s	bslt-s	feti-p	bslt-p	feti-h	and-1	and-1	and-s	and-s	feti-p	feti-1	feti-1	feti-1	and-s	and-h	and-1
% SiO ₂		50.6	50.4	50.9	51.5	50.9	52.7	51.4	51.5	59.4	58.1	56.5	57.0	51.4	51.5	51.4	50.7	56.6	56.3	56.1
TiO ₂		1.71	1.63	1.70	1.23	1.38	2.72	1.88	2.71	1.72	2.14	1.82	1.86	3.41	2.69	2.70	2.42	2.33	2.26	2.13
Al ₂ O ₃		13.2	13.3	13.1	14.3	13.7	12.3	12.5	12.3	10.2	10.2	10.8	11.2	11.1	11.9	12.0	12.5	11.3	11.0	11.3
FeO		12.8	12.2	12.9	10.8	11.3	15.5	13.0	15.4	15.0	15.7	15.7	15.6	17.6	15.3	14.8	14.8	14.9	15.1	14.9
MnO		0.21	0.22	0.22	0.21	0.21	0.22	0.22	0.36	0.26	0.27	0.27	0.27	0.28	0.24	0.26	0.24	0.25	0.30	0.24
MgO		16.9	16.83	16.87	7.67	7.82	3.78	6.26	5.28	1.56	2.02	1.63	1.52	3.50	4.71	5.80	10.1	7.16	6.51	7.51
NiO		0.11	0.10	0.11	0.05	0.05	0.11	0.11	0.11	0.19	0.19	0.19	0.19	0.21	0.25	0.25	0.25	0.25	0.25	0.25
K ₂ O		0.15	0.15	0.16	0.12	0.12	0.53	0.22	0.37	0.69	0.69	0.73	0.82	0.60	0.44	0.53	0.28	0.63	0.33	0.32
P ₂ O ₅		0.15	0.15	0.16	0.12	0.12	0.53	0.22	0.37	0.69	0.69	0.73	0.82	0.60	0.44	0.53	0.28	0.63	0.33	0.32
H ₂ O ⁺		0.15	0.16	0.16	0.12	0.12	0.53	0.22	0.37	0.69	0.69	0.73	0.82	0.60	0.44	0.53	0.28	0.63	0.33	0.32
C		0.15	0.16	0.16	0.12	0.12	0.53	0.22	0.37	0.69	0.69	0.73	0.82	0.60	0.44	0.53	0.28	0.63	0.33	0.32
Total		98.6	98.0	99.3	99.7	99.4	99.6	98.5	101.2	98.9	99.6	97.8	98.3	100.5	100.7	100.5	100.3	100.4	100.4	99.6
Ba		10	84	10	...	10	...	10	50	70	60	60	...	50	50	40	30	60	70	120
Ca		92	99	96	...	160	...	176	80	32	36	36	...	47	50	59	75	11	11	11
Mg		78	86	76	...	73	...	76	80	32	36	36	...	47	50	59	75	11	11	11
Ni		62	62	60	...	75	...	76	60	23	24	24	...	19	42	45	52	15	11	17
Cr		380	390	370	...	340	...	380	420	38	75	40	...	280	380	420	450	160	140	170
Zn		100	94	100	...	100	...	110	170	190	190	200	...	200	180	150	170	180	180	180
La		1	2	1	...	2	...	3	11	19	16	19	...	14	11	10	4	17	17	18
Sr		63	68	64	...	64	...	79	77	77	80	80
⁸⁷ Sr/ ⁸⁶ Sr		.702526	.702511	.702722	.702528702630	.702609	.702638703573

Notes:
 A: Microprobe analysis of glass from sheetflow surrounding active vents in "Rosa Gardens" area
 B: Microprobe analysis of glassy rind on blocky pillow west of alteration zone
 C: Microprobe analysis of glass from sample 52-5 D: Hornitic protruding from top of horst (approximately 0.5 m high)
 E: Hyaloclastite - slightly altered
 * not computed in corrections; FeO_T = residual FeO after pyrite correction; FeO_T = residual FeO; S as pyrite = pyrite sulfur except for 54-3A, 54-8r, where S was corrected for, and 54-5, 54-8r, where S was corrected for
 † relatively unaltered glassy interior analyzed by electron microprobe, moving beam method
 1. and = andesite, feti = Feti basalt, belt = MORB or ferrobasalt, ... = not analyzed, Bd = below glass
 2. p = massive or pillowed flow, l = lobate flow, s = sheet flow, h = hyaloclastite, alt = altered
 3. Major elements in percent, trace elements in ppm
 4. CO₂ < 0.1% in all samples; C indicates non-carbonate carbon
 5. Many of samples listed are located on Fig. 4
 6. Major element analyses by ICP-ES and electron microprobe trace elements by ICP-ES and C by wet-oxidation method
 7. Sr abundance determined by isotopic dilution techniques; ⁸⁷Sr/⁸⁶Sr measured on spiked samples at the University of Florida; all results are better than ± 0.00020 (2 sigma); measured values for NBS 987 during these analyses averaged 0.710234 ± 0.000010; Sr isotopes were normalized to ⁸⁷Sr/⁸⁶Sr = 0.1194

Locality		Alteration Zone: values corrected for Fe ₂ , CuS; i.e., S-free basis													
Sample No. DAVE/ATH.	Type	49-2A	49-2A1	49-2B	49-2C	49-2D	49-2E	54-8A	54-8B	54-8C	54-8L	55-1B	54-5	49-2B core	49-2B belt-1
		bslt-1	bslt-1	bslt-1	bslt-1	alt-h	alt-1	alt-h	feti-s	feti-s	and-p	alt-p	and-h	and-h	belt-1
% SiO ₂		56.7	63.9	46.7	44.7	43.3	38.1	33.8	68.0	64.4	70.0	31.6	56.7	51.8	51.8
TiO ₂		2.23	2.46	3.25	2.77	6.39	4.15	3.36	2.64	2.34	2.33	4.29	1.96	1.81	1.81
Al ₂ O ₃		12.0	11.3	17.5	15.1	18.5	20.2	17.5	11.6	11.5	11.0	20.3	9.65	13.7	13.7
FeO		13.08	9.64	17.08	15.0	16.9	18.4	22.2	10.9	12.6	10.4	17.8	20.5	13.9	13.9
MnO		7.58	2.91	6.97	6.98	13.2	10.5	11.1	3.85	3.06	3.04	0.11	0.09	0.16	0.16
MgO		2.32	0.51	1.66	2.76	1.11	2.54	0.22	0.88	0.77	0.47	1.66	0.61	0.61	0.61
CaO		1.23	0.72	1.41	1.62	2.56	1.99	0.33	0.95	0.74	0.78	1.52	0.57	3.23	3.23
Na ₂ O		0.00	0.09	0.04	0.02	0.29	0.14	0.07	0.18	0.13	0.17	0.15	0.12	0.15	0.15
K ₂ O		0.24	0.43	0.39	0.27	0.74	1.42	0.32	0.59	0.61	0.37	1.44	0.48	0.48	0.48
*S as py		4.1	14.0	9.15	7.22	30.5	6.63	12.0	10.0	7.85	9.70	11.9	2.1
*Fe as py		3.6	12.2	8.0	6.3	26.6	5.8	10.5	8.2	6.8	7.5	10.4	1.9
C		0.0	6.7	0.4	4.8	2.9	1.4	3.6	0.0	0.1	0.0	5.8	4.0
Total		99.8	99.4	99.6	96.0	100.2	93.5	93.9	98.8	96.7	98.2	93.6	94.7	100.9	100.9
Ba		89	11	126	109	58	12	13	13	12	12	82	12
Ca		869	9867	2520	1428	17400	3150	2055	...	4600	...	712	492
Ni		61	21	92	70	110	28	73	15	15	28	22	14
Zn		418	215	630	520	740	300	660	220	205	190	330	140
La		15	27	13	10	21	35	7	22	23	28	29	16
Sr		70637	...	705362	...	708262	708904	708391	...	708235
factor used		1.10	1.43	1.26	1.19	2.04	1.26	1.37	1.28	1.21	1.28	1.37	1.17

tered rocks that typically form cliffs and promontories. The inner alteration zone is well-defined by sharp transitions from soft, highly altered rocks to

harder, less fragmented and less altered rocks (Fig. 7d). These inner areas consist of a series of narrow anastomosing pipes or sheets of highly altered

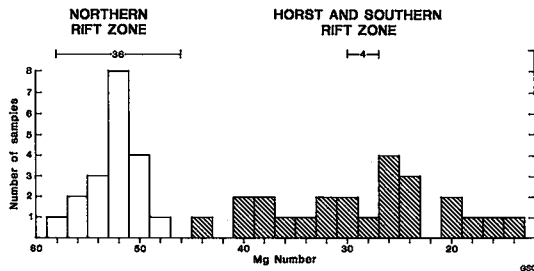


FIG. 6. Histograms of Mg-numbers for lavas from northern and southern valleys. Bars give range of Mg-numbers of MORB from 86°W, as calculated from Ballard *et al.* (1979); number of samples in each range is indicated.

materials (Fig. 7e), probably related to the positions of minor faults, flow-bedding planes and joints (Fig. 8).

Peripheral to the inner alteration zone, the closely fractured lavas commonly have red to yellowish coatings or stains primarily concentrated along fractures or parted intraflow surfaces (Fig. 7f). Microscopically, these are thin (<5 mm) palagonitized and ochrous zones within the fractured lavas or clay-silica coatings that washed off palagonitized surfaces. Chemical and petrologic comparisons of these "stained" samples with nearby fresh glass indicate that major and minor elements have not been affected by this type of "alteration", which is simply low-temperature precipitation (compare 1654-3A with 1654-6B, Table 1).

Meter-scale alteration channels locally breach the top of the horst; here sulfide mounds have formed. These channels terminate within several meters of the seafloor and form patches and layers of intensely altered material within well-preserved pillow lavas (Fig. 7d). Centimeter-scale conduits extend through the pillows, following local fractures and selvages up into the sulfide mounds on the top of the horst block (Fig. 8). The relatively unaltered nature of the lava flow covering part of the top of the horst is enigmatic (1654-3, Table 1). The trapped hydrothermal fluid may have been rapidly cooled through dilution with ambient seawater within a couple of meters of the seafloor. Less likely, a final extrusive event may have occurred after hydrothermal activity ceased.

The hydrothermal upflow zone encloses a complex stockwork of anastomosing veinlets whose density is controlled by the presence of fractures and extent of brecciation (Figs. 7i to 7l). Glassy andesitic pillows are fractured radially and have exfoliated (Fig. 7g). Basaltic sheet and lobate flows are fractured irregularly and along flow planes (Fig. 7i). Hyaloclastite beds have undergone pervasive invasion and alteration by hydrothermal fluids (Figs. 7d,l,m,n).

The veinlets are typically filled with a matrix of spheroidal, locally desiccated amorphous and cryptocrystalline silica either replaced or overgrown by Fe-rich chlorite, euhedral pyrite, chalcopyrite, cristobalite and minor sphalerite (Figs. 7i,k). Sulfide mineralization is largely restricted to the center of the upflow zone and occurs as veins and disseminations (Fig. 7j). In peripheral areas, fractures are much less dense and more typically filled with amorphous silica, amorphous hydrous iron oxides, and traces of iron-rich clay minerals.

Chemical analyses (Table 1) of rocks that enclose the alteration zone indicate that they are andesite, FeTi basalt and ferrobasalt. In the inner alteration zone, rocks were strongly depleted in Ca, Na, K, Mn, and enriched in S, Fe, Cu and Zn (*e.g.*, Fig. 9). Si is highly variable but also tends to be depleted; however, Al remained relatively immobile in all but the most altered samples. Mg is highly variable, showing local redistribution or addition leading to precipitation of chlorite on the margins of conduits, and almost total depletion in the cores of conduits. Ti and Al are unaffected even in highly altered lavas, and can be used as indicators of protolith composition.

Highly altered rocks comprise assemblages of smectite, silica (weakly crystalline cristobalite), minor chlorite and uncharacterized clay minerals, rutile or titanite, and "leucoxene". No primary plagioclase, augite, olivine, pigeonite, titanian magnetite or ilmenite are preserved. Most clay minerals are too fine-grained for microprobe analysis, but X-ray diffraction patterns, together with SEM-EDS analyses, are consistent with a chlorite/smectite mixture. Preliminary microprobe analyses of the mixed-layer clay minerals and chlorite indicate that both have a broad range of compositions, even within a single sample (Fig. 10). For example, sample 1649-2, from the center of the alteration zone, has a very iron-rich clay/chlorite assemblage in the most intensely sulfidic portion (sample 2a), but is quite magnesian away from this area (sample 2e). The Mg content of the clays seems to reflect the Mg content of the whole rock (Table 1). Pyrite, the most common sulfide, is finely disseminated in veinlets and their immediately adjacent wallrocks (Figs. 7j,k).

Less altered rocks that surround or flank the highly altered areas (Fig. 8) have preserved ilmenite cores within "leucoxene" (or titanite) envelopes; magnetite has been converted to hematite, and some plagioclase survives within clay envelopes. Intense alteration is restricted to within a few centimeters of fractures and is characterized by chlorite in the wallrocks immediately enclosing pyrite-cristobalite veinlets (Fig. 7i).

On a microscopic scale, alteration seems to have been controlled by episodic fluid movement through networks of fractures, because multiple layers of

differing mineral assemblages are arranged concentrically about fractures or fragment surfaces (Figs. 7i to 7l). Highly altered glassy pillows and interbedded hyaloclastite display intense fracturing and complex alteration zonation that is broadly and distinctively banded (Figs. 7m,n). However, mineral assemblages overlap considerably between adjoining zones. Further evidence for multi-phase alteration processes lies in rhythmic microlayering (mm to $<5\ \mu\text{m}$) (Figs. 7o,p) within broader (cm) layers of kaolinite-smectite-chlorite-cristobalite-sulfide, and multiple crack-seal structures within the veinlets themselves (Fig. 7k). Rocks from the surrounding outer alteration zone display only faint bleaching around thin fractures ($200\ \mu\text{m}$) or around vesicles; these may contain silica or an amorphous Fe-Ti oxide, according to microprobe and SEM-EDS analyses.

Strontium and oxygen isotopic analyses of a wide variety of fresh to highly altered rocks provide additional information about the conditions of alteration and mineralization in and around the stockwork zone (Smith *et al.* 1986, Smith 1987). Fifteen hand-picked and acid-cleaned glasses have $^{87}\text{Sr}/^{86}\text{Sr}$ values that range from 0.702511 to 0.702722, and $\delta^{18}\text{O}$ (relative to SMOW) from 5.5 to 6.2 (Table 1). Most of the samples, however, have Sr isotope ratios less than 0.702665 and $\delta^{18}\text{O}$ less than 5.9. These values are typical of fresh, normal (N-type) MORB from Pacific spreading centers (Ito *et al.* 1987, MacDougall & Lugmair 1986, White *et al.* 1987). In fact, the range of Sr isotope compositions of our sample set is even more restricted than those previously

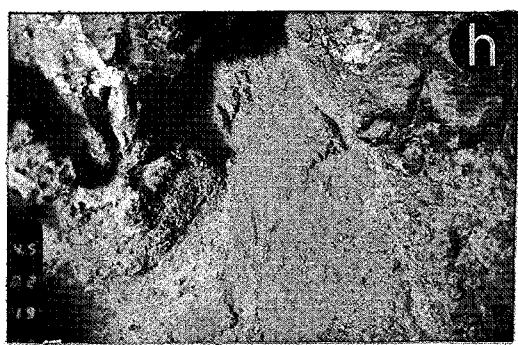
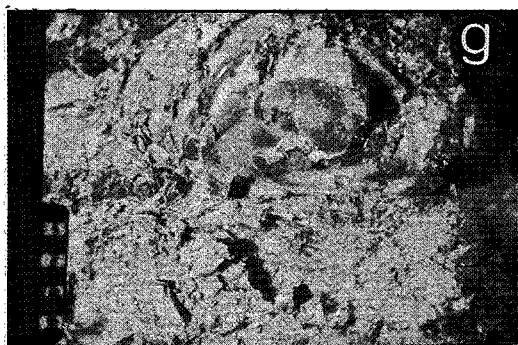
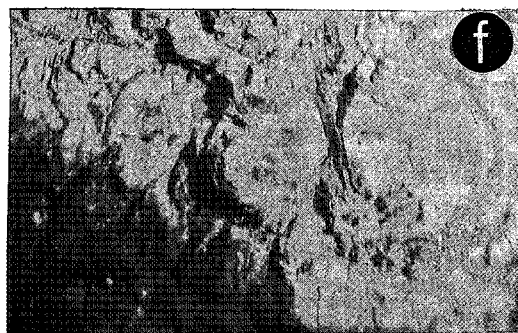
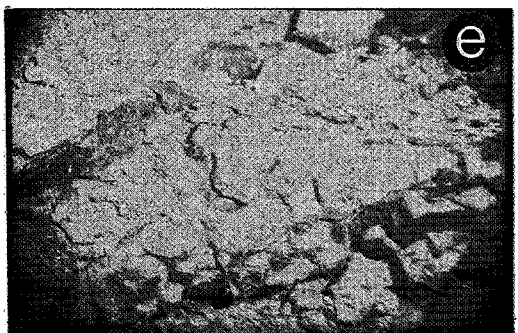
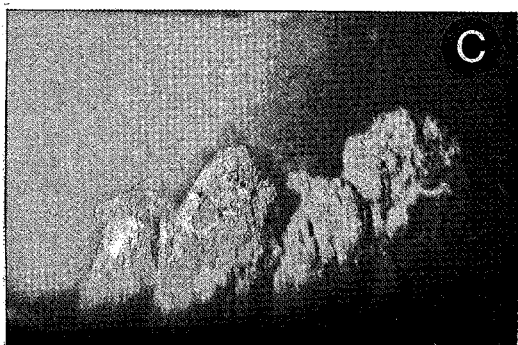
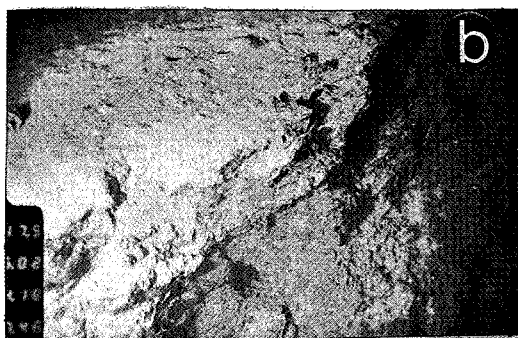
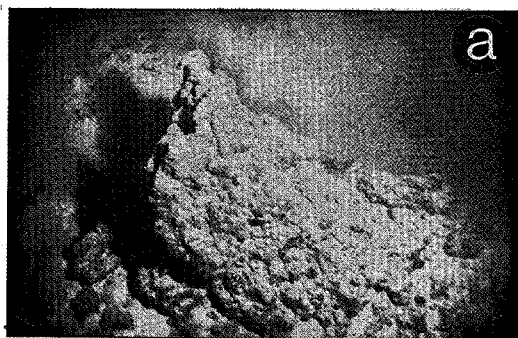
reported from the Galapagos Rift (Perfit *et al.* 1983, White *et al.* 1987), suggesting a fairly homogeneous source and little or no crustal contamination during magma evolution.

In contrast, 19 altered lava and hyaloclastite samples exhibit extremely variable Sr isotopic compositions (0.702678–0.708904, Table 1). Oxygen isotopic ratios in seven of these sample range from 6.6 in the least altered sample to a low of 3.9 in a highly altered and mineralized rock (Smith 1987). In general, the more altered a sample appears in thin section (*e.g.*, fewer relict minerals, more chlorite), the higher $^{87}\text{Sr}/^{86}\text{Sr}$ and lower $\delta^{18}\text{O}$ it has. Samples that have experienced only mild alteration (*e.g.*, clay replacement of primary phases, oxidation of mafic and oxide phases) have slightly elevated $^{87}\text{Sr}/^{86}\text{Sr}$ values and heavier ^{18}O relative to fresh samples (*e.g.*, sample 54-4, Table 1). Samples such as these are commonly described as “weathered” rather than hydrothermally altered. Samples of massive sulfide chimneys and Si-Mn-Fe mounds have the highest Sr isotope ratios (0.707080–0.709401).

Strontium concentrations in fresh lavas range from around 60 ppm in basalt to 80 ppm in andesite (Table 1). The weathered samples have similar to slightly elevated concentrations (80–100 ppm). Most of the hydrothermally altered and mineralized samples have Sr abundances less than 55 ppm. The lower concentrations correspond to depletions in Ca which can be related directly to the extent of feldspar destruction and accompanying chloritization of individual samples. Depletions in these elements can,

FIG. 7. (See following pages.) *Submersible-based photography.* (a) Weathered remnants of sulfide chimneys on south mounds (1651-1). Average compositions are given in Table 2. (b) Looking southwest into top edge of north wall (2536 m) near site 1654-6. Ten cm of sediment cover oxidized sulfide mound and underlying alteration zone. (c) Hyaloclastite pinnacles exposed on north cliff face 10 m below horst top (2547 m). Looking south near site 1654-4; slightly altered outer zone of pipe; field width about 4 m. (d) Oxidized sulfide (yellow) at contact of highly altered hyaloclastite (white) and relatively fresh glassy lobate flows (2546 m) near site 1654-4; field width about 2 m. (e) Closely fractured sheet flows display oxidized veins of iron-rich sulfides. Fractures are normal to layering. Near site 1654-8 (2542 m) north wall; field width about 1 m. (f) Glassy pillow lava is fractured, bleached and oxide-stained, especially along selvages. North wall looking south (2540 m); field width about 2 m. (g) Highly altered glassy pillow basalt (near 1654-4). Pronounced exfoliation and intensively fractured; selvages consist of soft clay and pyrite. North wall looking south (2540 m); pillow about 0.5 m. (h) Highly altered pillow andesite; sample 1654-8L was taken from space marked by a talus of pyritic sand (2542 m); field width about 1.5 m.

Hand specimens and photomicrographs: (i) Crackle breccia of partly altered ferrobasalt (1649-2C, Table 1) cemented by pyrite-cristobalite veinlets from inner zone of pipe (north wall, 2543 m). Alteration forms layers concentric to fractures, but is also localized on vesicles and certain flow layers. (j) Slab of highly altered pyritic stringer (1649-2A1) with pronounced alteration from white zones (kaolinite, silica, smectite) to green zones (chlorite, chlorite-smectite). (k) Stockwork veins show multiple crack-seal striping of pyrite-chalcocopyrite (black) and cristobalite (white). Glassy, microlitic ferrobasalt (1649-2A) from north wall of horst; field width 6.5 mm, plane light. (l) Chloritized andesitic hyaloclastite (1654-5) is cemented by cristobalite and sphalerite. Many shards are hollow. North wall at 2546 m. (m) As above; large brown sphalerite crystals in silica matrix (white). Patchy and variable alteration in glass. Field width 6.5 mm, plane light, crossed nicols. (n) As above; highly altered hollow fragments with concentric bands of chlorite, chlorite-smectite, silica. Interiors infilled with precipitates of similar compositions. Field width 6.5 mm, plane light, crossed nicols. (o) Highly magnified interior of large fragment in 7(n) displays micrometer-scale rhythmic precipitation of chlorite and silica; field width 1.7 mm, plane light. (p) SEM backscattered electron image of a single chlorite spheroid (upper right in 7o) shows rhythmic $5\ \mu\text{m}$ layering in a continuously grown crystalline matrix. Darker layers and spheres (SEM-EDS sites 3, 4, 6) are more Ti-rich and Fe-, Al-poor than white layers (as in site 2). Bright grains (5) are pyrite, grey band (1) is interpreted to be apatite.



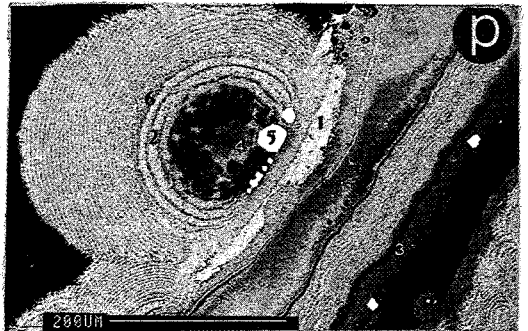
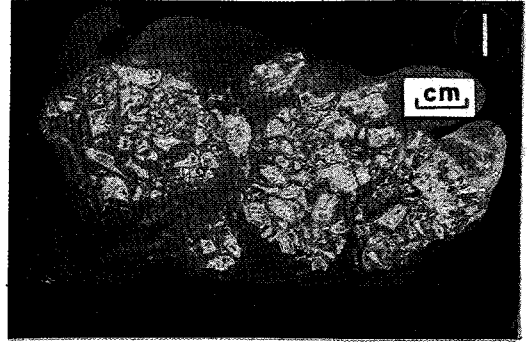
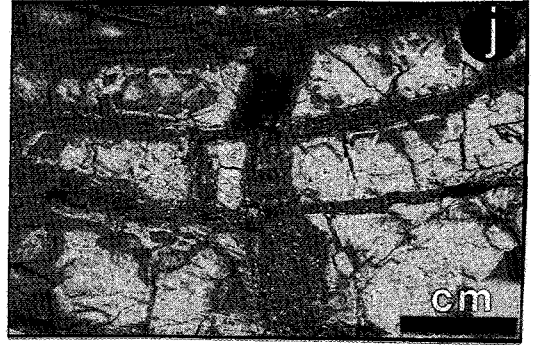
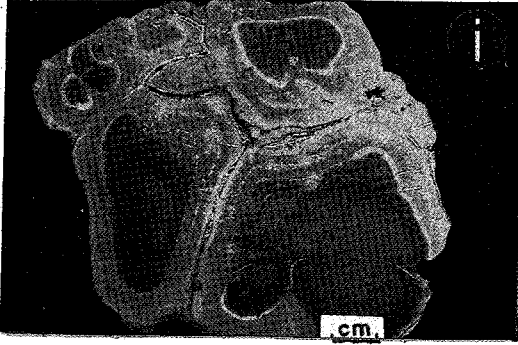


Table 2
Massive Sulfide Compositions

Dive	No. of samples	Cu (wt.%)	Zn (wt.%)	Fe (wt.%)	S (wt.%)	Pb (ppm)	Ag (ppm)	Au (ppb)
1646	3	2.17	0.23	16.6	31.6	104	11	66
1648	4	5.52	0.45	20.5	49.8	145	20	65
1649	1	0.41	0.07	45.5	54.9	180	12	91
1650	5	5.42	0.93	32.0	41.4	126	14	71
1651	2	6.90	2.44	29.4	49.3	240	33	143
1662	2	7.86	0.47	28.2	47.3	77	18	81
Averages all samples		4.7	0.8	28.7	45.7	145	17	80

1650 mounds: top of horst; all others: south base of horst and southern valley (Figure 4)

in part, be a result of dilution of the whole-rock Sr by the addition of Sr-poor sulfide minerals during hydrothermal alteration and mineralization, but seawater-rock interaction is likely the more dominant cause.

In general, there is an inverse relationship between Sr concentration and $^{87}\text{Sr}/^{86}\text{Sr}$ in the hydrothermally altered samples. A positive correlation exists in the weathered samples. In a few rocks that have discrete concentric zones of alteration (cm-scale), subsamples were drilled for isotopic analysis. The results showed that the highly chloritized zones (commonly on the rims or closest to mineralized veins) have the highest $^{87}\text{Sr}/^{86}\text{Sr}$ and lowest Sr ppm, both opposite to the least altered cores of the same samples. Intermediate zones, typically composed of mixed chlorite-smectite, have intermediate values. The Sr isotopic variations in individual samples parallel the trend observed in the whole rocks. It appears then, that macro-scale hydrothermal processes within the stockwork zone also occurred on a micro-scale within individual rocks.

The full results of our isotopic studies will be discussed elsewhere; however, our initial data provide some constraint on temperatures and water-rock ratios during alteration. Many studies have documented that increased $\delta^{18}\text{O}$ relative to mantle values (5.6–6.0) are the result of seawater alteration at low to moderate temperatures of 0 to $<200^\circ\text{C}$ (e.g., McCulloch *et al.* 1981, Barrett & Friedrichsen 1982, Stakes *et al.* 1983, Bohlke *et al.* 1984, Alt *et al.* 1986). Other studies have shown that low-temperature alteration or weathering by isotopically heavy seawater will effect modest increases in $^{87}\text{Sr}/^{86}\text{Sr}$ with little or no shift in Sr concentrations (Dasch *et al.* 1973, McCulloch *et al.* 1981, Spooner *et al.* 1977). In contrast, metamorphosed and highly altered rocks from the seafloor, particularly those associated with metalliferous deposits, have high $\delta^{18}\text{O}$ depletions and more radiogenic $^{87}\text{Sr}/^{86}\text{Sr}$

caused by interaction with hydrothermal fluids at temperatures $>300^\circ\text{C}$ (Vidal & Clauer 1981, Albarède *et al.* 1981, McCulloch *et al.* 1981, Alt *et al.* 1986).

The temperature-dependent fractionation of oxygen isotopes make $\delta^{18}\text{O}$ values extremely useful for determining temperatures of alteration, whereas the small mass differences between Sr isotopes makes them insensitive to temperature differences. Shifts in the Sr isotopic composition of oceanic rocks can, in the simplest sense, be considered a mixing process between unaltered igneous material and seawater or hydrothermal fluids (Spooner *et al.* 1974, McCulloch *et al.* 1981).

To determine the temperature and water-rock ratios operative in the fossil hydrothermal system we must assume the compositions of the end-members. Our data allow us to place fairly tight constraints on the composition of protoliths in the study area and the composition of seawater is well-known. We cannot, however, ignore the fact that as a hydrothermal system develops, the composition of the altering fluids must change as do the compositions of the crust through which they flow. Our results suggest that multiple pulses of fluids have affected some rocks in the stockwork zone, or that even small volumes of rock did not attain isotopic equilibrium. Relatively systematic changes in $^{87}\text{Sr}/^{86}\text{Sr}$, Sr ppm, and $\delta^{18}\text{O}$ in mineralogically zoned samples indicate that: (1) the composition of hydrothermal fluids could not have been much different than those measured in vents from the EPR at 21°N (Albarède *et al.* 1981), and (2) the isotopic values measured in whole rocks probably represent the integrated effects of hydrothermal alteration over the lifespan of the system.

Using the methods discussed by McCulloch *et al.* (1981) and Stakes & O'Neill (1982), alteration is estimated to have occurred from 150 to 320°C . The upper value is in good agreement with mineralogi-

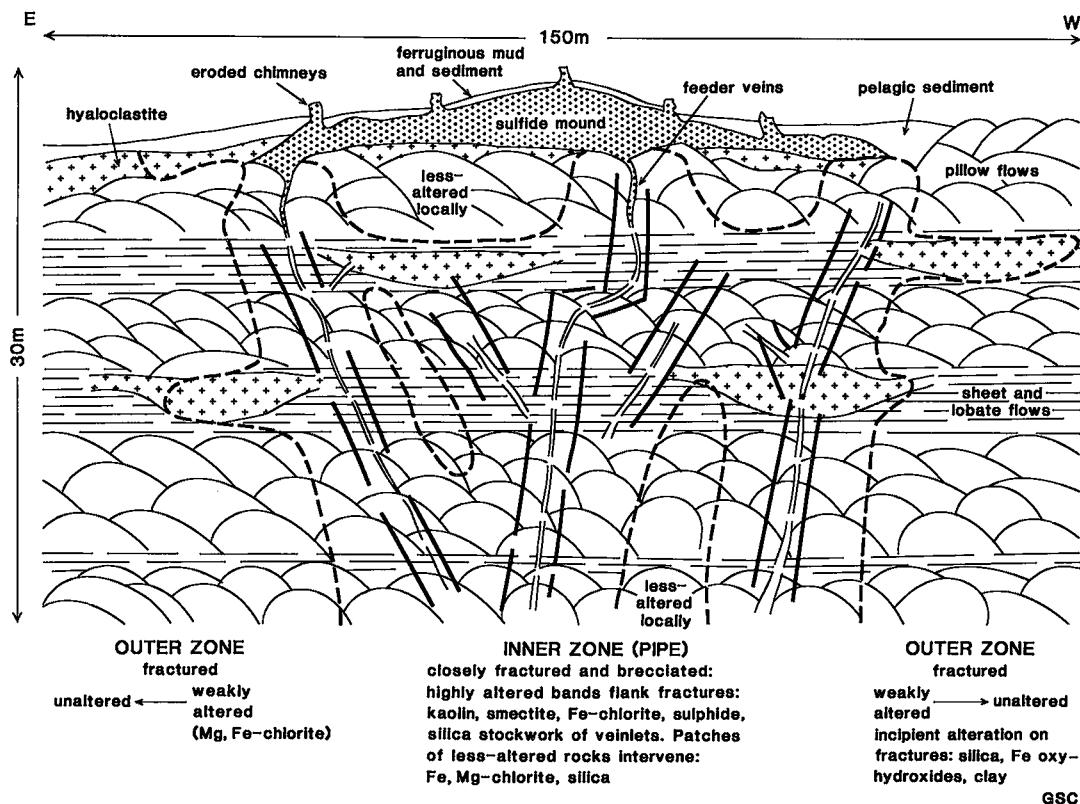


FIG. 8. Schematic section of the north wall (central horst) in the vicinity of the alteration zone, depicting structural and petrological features and their relationships to sulfide mounds. Reconstruction is based on visual observations, video, and still photography from ALVIN dives.

cal data and measured exit temperatures of fluids from active vent fields (Edmond *et al.* 1979, Delaney *et al.* 1984). A simple two-component mixing calculation using fresh Galapagos basalt and seawater as end-members roughly matches the variations in Sr and $^{87}\text{Sr}/^{86}\text{Sr}$ in altered samples (Smith 1987). Calculated water-rock ratios for whole-rock samples vary from 0.25:1 to 95:1, assuming perfect equilibrium mixing. In one of the concentrically zoned samples, calculated water-rock ratios vary from slightly greater than 1 in the least altered core to approximately 13 in the altered rim only 2 mm away. As the efficiency of exchange decreases, the calculated water-rock ratios will increase in a reciprocal manner. Consequently, if the mixing process was only 10% efficient, the water-rock ratios would be 10 times greater than those discussed above. In summary, it seems that the most highly altered and mineralized samples in the stockwork zone have interacted with large volumes of seawater-like hydrothermal fluids at $T \sim 300^\circ\text{C}$, and that multiple pulses of this hot fluid preferentially passed through small volumes of rock along closely spaced fractures that led to the seafloor.

MAGNETICS EXPERIMENTS

A deep-towed magnetometer profile was obtained across the rift valley at an altitude of 100 m above the seafloor to determine the presence and extent of magnetization anomalies generated by the sulfide deposits and the associated alteration zone. Magnetization lows had previously been detected over some continental hydrothermal areas, such as Wairakei (Studt 1959) and the Salton Sea (Koenig 1967), and also over some ancient massive sulfide deposits, as described by Johnson *et al.* (1982) for a deposit in the Troodos area of Cyprus. Similar anomalies have been detected over submarine hydrothermal areas (McGregor & Rona 1975, Phillips *et al.* 1969, Rona 1978). The marine studies, however, had been conducted using surface-towed magnetometers with receivers several km above the ocean floor. Our experiment was designed to place the receiver in close proximity to the seafloor, and centered over documented massive sulfide deposits.

The profile obtained from the submersible-mounted magnetometer was upward-continued to a level plane 2.2 km below the sea surface, and then

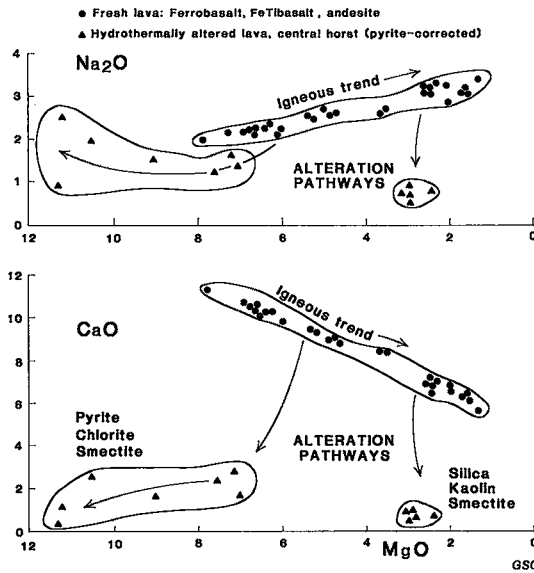


FIG. 9. Na_2O versus MgO plot (top) compares fresh and altered lavas from the central horst. Na_2O is strongly depleted in samples that have ferrobasalt and basaltic andesite protoliths. CaO versus MgO plot (bottom) shows similarly strong depletions in CaO .

was inverted for the magnetization solution (over a constant thickness layer of 500 m) using the Parker & Heustis (1974) Fourier inversion technique (Fig. 11). The profile shows a 4000-gamma anomaly located approximately 200 m north of the horst block that divides the survey area into two zones of relative magnetization. The northern valley has a relatively high magnetization compared to the horst block and southern valley (Fig. 11). A detailed submersible-based magnetometer survey also encountered the same magnetization contrast 200 m to the north of the horst. This corresponds to the position of the Neovolcanic Zone. The mapped sulfide deposits displayed no local anomalies, possibly because of their dominantly pyritic composition and their oxidized nature. The dramatic contrast in magnetization 200 m north of the horst is unlikely to be simply a function of age (*i.e.*, low-temperature alteration to maghemite and ultimately to titanite) since the age contrast is only of the order of a few thousand years. Petrologic differences between the northern and southern valleys are also unlikely to be the source of this contrast: FeTi basalt and andesite are as magnetic if not more so in comparison to MORB (*e.g.*, Vogt & De Boer 1976). The presence of pervasive alteration of Fe-Ti oxides and brecciation in the horst block area suggests that the magnetization contrast more likely reflects the presence of fresh unaltered crust in the northern valley and hydrothermally altered crust in the southern valley.

DISCUSSION

Petrochemical relationships

The striking spatial association of highly fractionated rocks and the sulfide deposit suggests the possibility of a genetic link. The coincidence of fractionated rocks and massive sulfide deposits has been demonstrated in other massive sulfide areas, such as Cyprus (Schminke *et al.* 1983). In other hydrothermal areas, notably along the EPR, little has been reported about the composition of the associated lavas. The significance of highly evolved lavas is twofold: 1) sulfur and volatile contents in FeTi basalt increase dramatically but sulfur decreases in the andesite; 2) small isolated magma chambers are required to create an environment conducive to extreme fractional crystallization (Perfit *et al.* 1983).

A decrease in sulfur content of andesite melt may have resulted either from immiscible separation of small amounts (<0.5 wt.%) of monosulfide liquid together with titanian magnetite micro-phenocrysts (Fornari & Perfit 1982, Perfit & Fornari 1983), or by degassing of sulfur from the magma. The former process would result in removal of most Ni, Cu and Co from the residual melt (Perfit *et al.* 1983, Clague *et al.* 1981). The separated sulfide liquid would, in this case, result in a portion of the subvolcanic cumulate enriched in monosulfide solid solution (*m.s.s.*) relative to most MORB-related subvolcanic intrusions.

Zinc does not partition as strongly into monosulfide liquid and would remain in similar amounts in andesite as in basalt (Shimazaki & MacLean 1976). Escape of S as a volatile phase would not be accompanied by depletion of involatile elements such as Cu from andesite. Moreover, low vesicle contents and high volatile concentrations (H_2O , Cl, F) do not indicate de-gassing (Perfit *et al.* 1983). Preliminary analyses (Table 1) indicate that andesite samples have only half the Cu content of most of the basalt samples. Petrographic observations confirm the presence of tiny *m.s.s.* droplets, closely associated with magnetite, in the andesite.

The presence of highly evolved lavas on the Eastern Galapagos Rift suggests extensive crystallization of small magma bodies (<30 km^3) at depths less than 2 km beneath the seafloor (Perfit *et al.* 1983). These magma chambers provide heat to localized hydrothermal systems, enabling them to attain temperatures of at least 350°C; such systems probably exist for less than 10,000 years (Cann *et al.* 1985/1986). These ephemeral chambers may develop as small cupolas above larger steady-state magmatic reservoirs that may be related to relatively small offsets in the ridge crest (DEVALs of Langmuir *et al.* 1986, OSCs of Macdonald *et al.* 1984). Along the Eastern Galapagos Rift, development of these shallow intrusions seems to be enhanced by the thermal effects of rift propagation (Fornari *et al.* 1983, Per-

fit *et al.* 1983). In contrast, where sub-rift chambers are continually replenished, erupted basalts are more mafic and uniform in composition; this may be the situation in the Neovolcanic Zone (north valley). Langmuir *et al.* (1986) have recovered similarly highly fractionated lavas only at DEVALs along the northern EPR. A crucial test of this genetic model linking fractionation processes to massive sulfide generation on the seafloor will result either from more exploration for sulfides in areas of fractionated lavas, or through a more thorough assessment of petrographic trends in lavas associated with major seafloor-sulfide deposits.

Sulfide compositions

The most striking aspect of the sulfides in the Galapagos mounds is their copper-rich composition (Cu:Zn 6:1; Table 2) in comparison with other seafloor deposits (Cu:Zn ~0.1; Bischoff *et al.* 1983, Kappel & Franklin 1988). As with all of the volcanic-associated deposits on the modern seafloor, these are within the Cu-Zn group (Franklin *et al.* 1981). The Galapagos deposits are similar to sulfides on an off-axis seamount at 12°N (Hékinian & Fouquet 1985), to the deposits at Cyprus, and to the Cu-rich portions of many ancient deposits (Franklin *et al.* 1981). At least two mechanisms can explain the Cu-rich nature: 1) the fluids were relatively Cu-rich compared with fluids in active vent sites, either through some peculiarity in the source region, or 2) through fractional precipitation of Cu minerals from the ascending hydrothermal fluid, either in the zone of ascent or within the sulfide mound.

Although the source region cannot yet be examined, the dykes and lavas that comprise the lower part of the oceanic crust are most probably represented by the rocks at surface. Perfit & Fornari (1983) noted an increase in Cu content from MORB through ferrobasalt to FeTi basalt, the dominant rock type. Zinc content of all types is constant. The relatively Cu-rich FeTi basalt may have provided more Cu to the hydrothermal fluid, but as the Cu:Zn ratio increases from only 1 in MORB to about 1.5 in the FeTi basalt, using the simplistic explanation of metal content of the source rocks to explain the large difference in sulfide compositions is not adequate. As demonstrated experimentally by Seyfried & Janecky (1985), the metal content of a hydrothermal fluid is obtained only where the pH is sufficiently acid to promote chloride-ion complexing; this acidity is reached in basalt at about 385°C, and the metal content of the fluid is more or less independent of rock composition at that point. Thus, although it cannot be ruled out, variation in metal content of the source rocks is not a likely explanation for the high Cu content at Galapagos. The high content of sulfur (as *m.s.s.*) in the FeTi basalt, however, may have resulted in an exceptionally

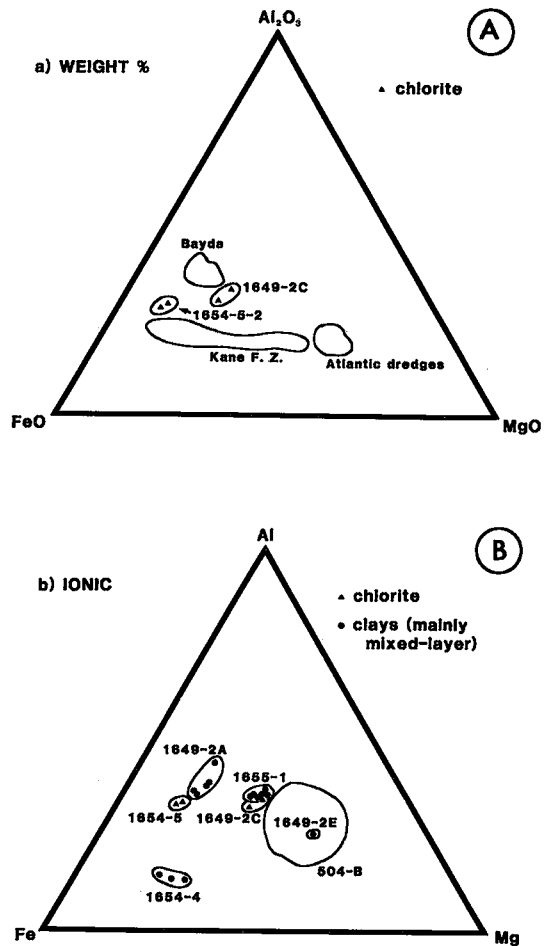


FIG. 10. Preliminary analyses of chlorite and smectite minerals from the central area of alteration (Fig. 8). (A): composition of chlorite from tow samples, with comparative data for the Mid-Atlantic Ridge (Humphris & Thompson 1978); Kane Fracture Zone (Delaney *et al.* 1987); Bayda massive sulfide deposit, Oman (Collinson 1986). (B): compositions (mole proportions) of chlorite (triangles) and (mainly mixed-layer) clays (circles) from the central part of the alteration zone. Field for Hole 504B chlorite/smectite compositions from Alt *et al.* (1986). All analyses by wavelength dispersion microprobe techniques.

sulfur-rich hydrothermal fluid.

Fractional precipitation of Zn relative to Cu within the zone of ascent can be ruled out, as the sulfides in both the Galapagos alteration pipe and in ancient alteration pipes are all Cu-rich. Furthermore, as demonstrated by many solubility calculations (see Franklin *et al.* 1981 for summary), Cu precipitates preferentially from a high-temperature hydrothermal fluid. Copper minerals are thus most abundant in the stringer zone, and the remaining fluid is relatively

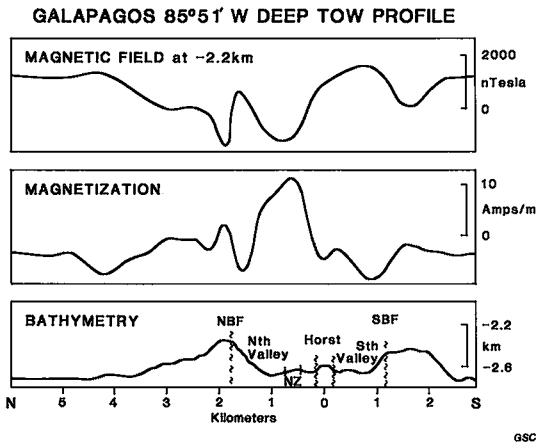


FIG. 11. Deep-tow magnetometer profile over study area. Location in Figure 2. Top profile is the upward continued magnetic field at a level of 2.2 km below sea-level. The magnetization profile (center) was computed using a Fourier inversion technique.

Zn-rich. Similarly, zone refining takes place within the chimney and mound structures, with Cu precipitated in the high-temperature chimney linings, and Zn precipitated in the lower temperature outer portions (Haymon & Kastner 1981), or lost altogether. It may be this last process, taken to completion in mature systems such as Galapagos, that explains the Cu-rich composition. As hydrothermal fluid moved through the well-established mounds at Galapagos, the cooling high-temperature fluid probably diffused outward, causing dissolution of sphalerite and replacement by copper minerals. As the mounds heated, they became more Cu-rich.

Alteration assemblage

The petrographic and submersible observations provide some new insights into the alteration process and timing of hydrothermal activity. Alteration channels cut the entire lava sequence, so hydrothermal activity must have been initiated near the end of volcanic activity, and continued afterward. Although hydrothermal activity probably accompanied volcanism (*cf.* Rise Project Group 1980), the most prolific period of sulfide formation post-dated local volcanism. This observation is consistent with those made at the Endeavor Ridge (Kappel & Franklin 1988) and the 12°N seamount (Hékinian & Fouquet 1985). Evidently the optimum time of formation of large seafloor massive sulfide deposits is immediately following, and not during, the culminating volcanic event in any specific portion of a ridge crest.

The mineral assemblage, dominated by smectite, cristobalite, amorphous silica, pyrite and minor chlo-

rite, is consistent with metasomatic alteration that originated from both high-temperature fluid and locally-warmed seawater. Iron-rich minerals must have precipitated from the hydrothermal fluid, but the more magnesian minerals may have formed due to interaction with locally derived seawater as metaliferous hydrothermal fluids are notoriously deficient in Mg (Edmond *et al.* 1979). The delicate concentric rhythmic layering of alteration minerals may indicate a repetitive change in the flux of hydrothermal fluid. Crack-seal veins indicate that, at least for short periods, the fluid pressure exceeded the lithostatic load. The large variation in Fe/Mg ratio of the clay/chlorite assemblages, even within single samples, indicates that alteration involving direct interaction with the hydrothermal fluid may have gone on immediately adjacent to the major fluid channelways. Within a few cm of the channelways, rapidly heated, locally derived seawater was contemporaneously reacting with the basalt.

The loss of alkalis, and strontium isotope data, indicate that the water-rock ratio was very high in the alteration core, consistent with observations in preserved deposits (Mottl 1983, Roberts & Reardon 1978). The general increase in $^{87}\text{Sr}/^{86}\text{Sr}$ with intensity of alteration indicates that much of the alteration formed from reaction with something other than the ascending metalliferous fluid. Several studies (*e.g.*, Hinkley & Tatsumoto 1987) have shown that the Sr isotopic composition of unmodified hydrothermal fluid is close to that of the host basalt. The high $^{87}\text{Sr}/^{86}\text{Sr}$ compositions must have been generated from reaction with advecting, locally derived seawater.

The range of temperatures calculated from the oxygen isotopic data are consistent with highly variable mineral assemblages associated with the wall-rocks to the stockwork veins. Both progressively heated local seawater and cooled hydrothermal fluid could produce this range of temperatures. Magnesian clays must have originated from interaction with advecting seawater, or by redistribution of Mg from the zone of interaction of hydrothermal fluid immediately adjacent to the stockwork veins.

In summary, the mineralogical and isotopic data indicate that a large volume of locally derived seawater had a major role in producing the alteration within the basalt. The vein fillings (silica, pyrite) and alteration products in their immediate wallrocks were obtained, however, primarily from the metalliferous hydrothermal fluid.

COMPARISON WITH OTHER HYDROTHERMAL SYSTEMS

The presence of alteration halos around massive sulfide orebodies has long been recognized as an important exploration tool. Franklin *et al.* (1981), Franklin (1986), and Morton & Franklin (1987)

presented compositional classifications of massive sulfide deposits and suggested that genetic relationships exist between the type of alteration and the environment of formation of these deposits. Under the above classification schemes most of the ridge-crest deposits are the "Cu-Zn" type. The Galapagos alteration zone is an excellent example of a totally unmetamorphosed and undeformed alteration zone; the characteristics of such examples are the basis for interpreting preserved pipes throughout the geological record, and are of great significance in establishing an ever more precise genetic model for massive sulfide deposits. It is thus important to establish the amount of similarity between the Galapagos pipe and alteration under major ancient deposits.

The sulfide deposits within the Abitibi greenstone belt of northern Quebec and Ontario are some of the largest and best studied of the Cu-Zn class. They are in bimodal (basalt and rhyolite) sequences in which mafic rocks predominate. Detailed models of alteration pipes typical of this area are available for the Mattagami Lake mine in northern Quebec. Roberts & Reardon (1978) and Costa *et al.* (1983) have identified the following alteration trends: (1) removal of Na and K, (2) addition of Mg, Mn and Fe (in chlorites), (3) removal of silica to produce chlorite-rich rock, and (4) late potassic alteration coupled with transformation of chlorite to phlogopite.

The basic model of Costa *et al.* (1983) suggests that heat flow associated with a magmatic source has induced a thermally driven convective flow system whereby ambient seawater was drawn into the rising hydrothermal fluid. Furthermore, the highest Mg concentrations commonly are in the upper and outer parts of the pipe, where a high flux of locally warmed seawater through the country rocks interacted with the lavas to produce Mg-enriched chlorite. As the zone of high flux of hydrothermal fluid in the core of the pipe is approached, the Mg available from cold ambient seawater decreased and the relatively reduced, iron-rich fluids reacted with the volcanic rock to produce Fe-rich chlorite. Therefore, in the most simplistic case, the Fe:Mg ratio would increase towards the center of the alteration pipe. However, as Costa *et al.* (1983) and Franklin (1986) point out, the Fe:Mg ratio in any given system probably depends on the total flux and the rate of discharge, which directly relate to the amount of mixing with cold seawater and consequent overprinting of a "primary" Fe chlorite-rich core alteration zone by later Mg-rich chlorite. The Galapagos alteration zone generally conforms to this model, with Fe metasomatism more dominant in the center of the alteration zone, and Mg metasomatism more dominant outside. The Mattagami deposit, however, has much more Mg alteration than Galapagos.

The Cu-Zn massive sulfide deposits that formed

in tectonic settings most analogous to the Galapagos sulfides are those in ophiolite complexes. The best documented ophiolitic stockwork zones are in Oman and Cyprus. The Bayda deposit in Oman occurs in a pillow-lava sequence of the Semail ophiolite interpreted by Alabaster & Pearce (1985) as part of an off-axis seamount province on the flank of a marginal ocean-basin spreading center. As at Galapagos, the stockwork zone consists mostly of quartz, plus Fe-rich chlorite and pyrite veinlets within highly fractured wallrocks. Collinson (1986) outlined four alteration stages, *viz.*, quartz + hematite; quartz + pyrite (main stage); quartz + chlorite; quartz + hematite (late stage). The earliest and latest stages of alteration have not been recognized at Galapagos, implying that the brecciation-hydrothermal flow events were triggered and terminated abruptly. At Galapagos, heated seawater was unable to mix and react with hydrothermal fluid in the central zone of the alteration pipe. However, a peripheral zone of silica + hydrated iron oxides on the margins of the pipe indicates that some shallow downwelling and mixing did take place on the flanks of the upwelling zone, but this formed only minimal, superficial alteration along fractures (contrast with Bayda where peripheral alteration is more pervasive: hematite + albite + quartz + zeolites). The preservation of cristobalite and cryptocrystalline silica rather than chalcedonic quartz throughout the inner alteration zone at Galapagos supports the concept of very little post-alteration fluid flow. Silica gel formed by super-cooling (quenching) first forms alpha cristobalite and would anneal very slowly at low temperature (ambient seawater) to alpha quartz (Plyusnina 1984). The similarity in style of the main stages at the two sites is further emphasized by similarly high Fe:Mg chlorites and common mineral assemblages.

The stockwork zones at Mathiati and Kokinopezoula in Cyprus (Lydon & Galley 1986, Richards *et al.* 1988) are similar to Galapagos in alteration-mineral assemblages and chemical composition. The Mathiati deposit in particular is an excellent analog to Galapagos in all respects, including chlorite compositions (Lydon & Galley 1986). The basic mineralogical and chemical changes in alteration zones at Mathiati, Bayda, and Galapagos are similar; all have undergone loss of Ca and Na, massive precipitation of silica, and the formation of Fe-rich chlorite.

In contrast, stockwork alteration zones not overlain by exhalative massive sulfides (DSDP Site 504B, Mid-Atlantic Ridge and the Pitharkhoma deposit of Cyprus) show somewhat different chemical characteristics (Alt *et al.* 1986, Richards *et al.* 1988, Fig. 10). As at Galapagos, the stockwork zone in Hole 504B contains sulfide stringers in quartz veinlets, and displays evidence of multiple mineralizing events (Honnorez 1981, Honnorez *et al.* 1985).

However, Hole 504B stockwork is enriched in alkalis, whereas Galapagos is strongly depleted. The alteration described by Delaney *et al.* (1987) for Mid-Atlantic Ridge greenstone is also similar; there, chlorite has a high Fe:Mg ratio that distinguishes it from other seafloor metabasalt. Delaney *et al.* interpret the chlorite alteration as a product of a highly evolved, high-temperature, high-salinity fluid moving through a hydrothermal upflow zone.

It is important to note that massive sulfide deposits and stockwork zones are commonly associated with highly evolved lavas in ancient greenstone belts and in some ophiolites, similar to the exceptional association with andesite and FeTi basalt at Galapagos. Most of the lavas in the Troodos extrusive sequence are basaltic andesite or andesite (Schmincke *et al.* 1983) and range up to rhyodacite (Robinson *et al.* 1983). Similar andesitic lavas and shallow-level differentiated plutonic rocks (plagiogranites) have been described near alteration zones in the Semail ophiolites (Alabaster *et al.* 1979). Campbell *et al.* (1982) have demonstrated anomalous fractionation histories for felsic volcanic rocks associated with several massive sulfide districts in the Precambrian Shield. They attribute these to very efficient cooling of high-level subvolcanic magma chambers by heat transfer into a hydrothermal system. Thus, the determination of such anomalous petrogenetic trends both in felsic and mafic sequences can be an important guide to new resources.

CONCLUSIONS

(1) The Galapagos sulfide mounds at 85°50.5' W were formed several thousands of years ago during a hydrothermal episode associated with faulting along a horst-type structure. The horst separates a southern rift valley from a northern rift valley that contains the Neovolcanic Zone.

(2) The lavas in the Neovolcanic Zone are average MORB, whereas those from the horst and the southern valley range from evolved MORB to andesite. The extreme differentiation necessary to produce this cogenetic suite of volcanic rocks probably resulted from cooling of a small, shallow magma chamber. Heat from this magma enabled the development of a large volume of metalliferous hydrothermal fluid at a shallow crustal depth. Evidence for such anomalous fractionation of high-level magma chambers has been noted in Precambrian sequences (Campbell *et al.* 1982), and may be a key exploration guide.

(3) The unusual nature of the double rift valley is also reflected in the magnetic-field data. The highly magnetic northern rift valley has a magnetic expression that contrasts with the less magnetic horst block and southern rift valley. This magnetization contrast probably reflects limited or no hydrothermal alter-

ation in the northern valley, but pervasive hydrothermal alteration in the mineralized horst and underlying the southern valley.

(4) The stockwork-like zone exposed on the scarp directly beneath the massive sulfide mounds on the north side of the horst is similar in general form and character to those associated with ophiolite-hosted massive sulfides, in particular those in Cyprus and Oman. The amount of alteration is directly proportional to permeability, *e.g.*, hyaloclastites are totally altered to clays, whereas pillow-lava alteration is controlled by pre-existing fractures with less alteration occurring in a zoned pattern inward from silica- and sulfide-filled fractures. Layering represents a hitherto unknown pulsation in a hydrothermal system.

Altered rock is extremely depleted in Ca, K and Na, and enriched in Fe²⁺ and S. Mg and Si contents are variable, indicating different amounts of mixing of hydrothermal fluid and seawater within the alteration zone. Chemical and isotopic data indicate that large volumes of locally derived, progressively heated seawater, advecting near the upwelling zone, were responsible for much of the alteration. Alteration directly effected by the metalliferous hydrothermal fluid is confined to the immediate zones of fluid upwelling.

The Galapagos sulfide site is the first example where the relationships between alteration and sulfide accumulation can be studied in the absence of modification by post-depositional thermal and deformational effects. With exhaustive study it will provide further new insights into the mineralization process.

ACKNOWLEDGEMENTS

We are grateful to Susan Hanneman, who worked tirelessly on all aspects of the data collection and on the laborious and frustrating task of piecing together the dive data. Chris Fox and Joyce Miller devoted considerable time and effort to merging the Sea Beam and SASS multibeam bathymetric data sets and we thank them and the URI Sea Beam group for their efforts. All of the *ATLANTIS II* ship and scientific complement, in particular Michael Jackson, Tetsuro Urabe, Stan Jones, Lowell Fritz and Makoto Yuasa contributed to the success of the dive series. We thank Harald Bäcker and members of the FS *SONNE* for their valuable on-site collaboration. The success of our dives reflects the dedication and professionalism of the pilots, technicians and office staff responsible for the submersible, and we heartily thank pilots Ralph Hollis, Dudley Foster, William Sellers and the rest of the ALVIN group for their efforts. We gratefully acknowledge the support of the NOAA Office of Undersea Research for financial support of the dive series. Rachel Haymon provided valuable discussion and information on the Oman stockwork zone. At the Geological Survey of

Canada, Gwendy Hall and Gerry Lachance supervised geochemical analyses, Gina LeCheminant provided microprobe data on sulfide and clay minerals, Adrienne Larocque carried out XRD determinations of clay minerals, and David Walker supplied SEM analyses.

At the University of Florida, R. Shuster provided analytical expertise on samples prepared by M. Lebron. The analytical work has been supported in part by the U.S. Department of Commerce (NOAA-50ABNR-7-00131) and the National Science Foundation (OCE 87 16827).

REFERENCES

- ALABASTER, T. & PEARCE, J.A. (1985): The interrelationship between magmatic and ore-forming hydrothermal processes in the Oman ophiolite. *Econ. Geol.* **80**, 1-16.
- , PEARCE, J.A., MALLICK, D.I.J. & ELBONSHI, I.M. (1979): The volcanic stratigraphy and location of massive sulphide deposits in the Oman ophiolite. *In Ophiolites: Proc. Int. Symposium 1979*, Cyprus (A. Parayiotou, ed.). *Cyprus Ministry of Agriculture, Natural Resources and Geology, Geol. Surv. Dep.*, 751-757.
- ALBAREDE, F., MICHARD, A., MINSTER, J.F. & MICHARD, G. (1981): $^{87}\text{Sr}/^{86}\text{Sr}$ ratios in hydrothermal waters and deposits from the East Pacific Rise at 21°N. *Earth Planet. Sci. Lett.* **55**, 229-236.
- ALT, J.C., HONNOREZ, J., LAVERNE, C. & EMMERMANN, R. (1986): Hydrothermal alteration of a 1-km section through the upper oceanic crust, Deep Sea Drilling Project Hole 504B: Mineralogy, chemistry, and evolution of seawater-basalt interactions. *J. Geophys. Res.* **91**, 10309-10336.
- BÄCKER, H., LANGE, J. & MARCHIG, V. (1985): Hydrothermal activity and sulphide formation in axial valleys of the East Pacific Rise crest between 8° and 22°S. *Earth Planet. Sci. Lett.* **72**, 9-22.
- BALLARD, R.D., HOLCOMB, R.T. & VAN ANDEL, T.H. (1979): The Galapagos rift at 86°W, 3. Sheet flows, collapse pits and lava lakes of the rift valley. *J. Geophys. Res.* **84**, 5407-5422.
- , VAN ANDEL, T.H. & HOLCOMB, R.T. (1982): The Galapagos Rift of 86°W: Variation in volcanism, structure and hydrothermal activity along a 30-kilometer segment of the rift valley. *J. Geophys. Res.* **87**, 1149-1161.
- BARRETT, T.J. & FRIEDRICHSEN, H. (1982): Strontium and oxygen isotopic composition of some basalts from Hole 504B, Costa Rica Rift, DSDP Legs 69 and 70. *Earth Planet. Sci. Lett.* **60**, 27-38.
- BISCHOFF, J.L., ROSENBAUER, R.J., ARUSCAVAGE, P.J., BAEDCKER, P.A. & CROCK, J.G. (1983): Sea-floor massive sulfide deposits from 21°N, East Pacific Rise; Juan de Fuca Ridge; and Galapagos rift. Bulk chemical composition and economic implications. *Econ. Geol.* **78**, 1711-1720.
- BOHLKE, J.K., ALT, J.C. & MUEHLENBACHS, K. (1984): Oxygen isotope - water relationships in altered deep-sea basalts: low temperature mineralogical controls. *Can. J. Earth Sci.* **21**, 67-77.
- BONATTI, E., GUERSTEIN-HONNOREZ, B.M. & HONNOREZ, J. (1976): Copper-iron sulfide mineralizations from the equatorial Mid-Atlantic Ridge. *Econ. Geol.* **71**, 1515-1525.
- CAMPBELL, I.H., COAD, P., FRANKLIN, J.M., GORTON, M.P., SCOTT, S.D., SOWA, J. & THURSTON, P.C. (1982): Rare earth elements in volcanic rocks associated with Cu-Zn massive sulphide mineralization: a preliminary report. *Can. J. Earth Sci.* **19**, 619-623.
- CANN, J.R., STRENS, M.R. & RICE, A. (1985/86): A simple magma-driven thermal balance model for the formation of volcanogenic massive sulphides. *Earth Planet. Sci. Lett.* **76**, 123-134.
- CLAGUE, D.A., FREY, F.A., THOMPSON, G. & RINDGE, S. (1981): Minor and trace element geochemistry of volcanic rocks dredged from the Galapagos spreading centre: Role of crystal fractionation and mantle heterogeneity. *J. Geophys. Res.* **86**, 9469-9482.
- COLLINSON, T.B. (1986): *Hydrothermal Mineralization and Basalt Alteration in Stockwork Zones of the Bayda and Lasail Massive Sulfide Deposits, Oman Ophiolite*. M.A. thesis, Univ. California, Santa Barbara, California.
- CORLISS, J.B., DYMOND, J., GORDON, L.I., EDMOND, J.M., VON HERZEN, R.P. & VAN ANDEL, T.H. (1979): Submarine thermal springs on the Galapagos Rift. *Science* **203**, 1073-1083.
- COSTA, V.R., BARNETT, R.L. & KERRICH, R. (1983): The Mattagami Lake Mine Archean Zn-Cu sulfide deposit, Quebec: Hydrothermal coprecipitation of talc and sulfides in a seafloor brine pool - evidence from geochemistry, $^{18}\text{O}/^{16}\text{O}$ and mineral chemistry. *Econ. Geol.* **78**, 1144-1203.
- DASCH, E.J., HEDGE, C.E. & DYMOND, J. (1973): Effect of seawater interaction on strontium isotope composition of deep-sea basalts. *Earth Planet. Sci. Lett.* **19**, 177-183.
- DELANEY, J.R., McDUFF, R.E. & LUPTON, J.E. (1984): Hydrothermal temperatures of 400°C on the Endeavor segment, northern Juan de Fuca Ridge. *EOS, Trans. Amer. Geophys. Union* **65**, 973.
- , MOCK, D.W. & MOTT, M.J. (1987): Quartz-cemented, sulfide-bearing greenstone from Mid-Atlantic Ridge; sample of a high-temperature, high-salinity hydrothermal upflow zone. *J. Geophys. Res.* **92**, 9175-9192.

- EDMOND, J.M., MEASURES, C., MANGUM, B., GRANT, B., SCLATER, F.R., COLLIER, R., HUDSON, A., GORDON, L.I. & CORLISS, J.B. (1979): On the formation of metal-rich deposits at ridge crests. *Earth Planet. Sci. Lett.* **46**, 19-30.
- FORNARI, D.J. & PERFIT, M.R. (1982): Sulfide fractionation: its role in the evolution of massive sulfide deposits along the mid-ocean ridge crest. *EOS, Trans. Amer. Geophys. Union* **63**, 1135.
- _____, _____, MALAHOFF, A. & EMBLEY, R.W. (1983): Geochemical studies of abyssal lavas recovered by DSRV ALVIN from eastern Galapagos rift, Inca transform and Ecuador rift, 1. Major element variations in natural glasses and spatial distribution of lavas. *J. Geophys. Res.* **88**, 519-530.
- FRANKLIN, J.M., (1986): Volcanic-associated massive sulphide deposits, an update. In *Geology and Genesis of Mineral deposits in Ireland. Irish Assoc. Econ. Geol. Spec. Vol.* (C.J. Andrew, R.W.A. Crowe, S. Finlay, W.M. Pennel & J.F. Pyne, eds.), 49-69.
- _____, LYDON, J.W. & SANGSTER, D.F. (1981): Volcanic-associated massive sulfide deposits. *Econ. Geol. 75th Anniv. Vol.*, 485-627.
- HAYMON, R.M. & KASTNER, M. (1981): Hot spring deposits on the East Pacific Rise at 21°: preliminary description of mineralogy and genesis. *Earth Planet. Sci. Lett.* **53**, 363-381.
- HÉKINIAN, R. & FOUQUET, Y. (1985): Volcanism and metallogenesis of axial and off-axial structures on the East Pacific Rise near 13°N. *Econ. Geol.* **80**, 221-249.
- HINKLEY, T.K. & TATSUMOTO, M. (1987): Metals and isotopes in Juan de Fuca Ridge hydrothermal fluids and their associated solid materials. *J. Geophys. Res.* **92**, 11400-11410.
- HONNOREZ, J. (1981): The aging of oceanic crust at low temperature. In *The Sea 7* (C. Emiliani, ed.). John Wiley & Sons, New York.
- _____, ALT, J.C. HONNOREZ-GUERSTEIN, B.-M., LAVERNE, C., MUEHLENBACHS, K., RUIZ, J. & SALTZMAN, E. (1985): Stockwork-like sulfide mineralization in young oceanic crust. In *Initial Reports Deep Sea Drilling Project 83*, 263-282. U.S. Gov. Printing Office, Washington, D.C.
- HUMPHRIS, S.E. & THOMPSON, G. (1978): Hydrothermal alteration of basalt by seawater. *Geochim. Cosmochim. Acta* **42**, 127-145.
- ITO, E., WHITE, W.M. & GOPEL, C. (1987): The O, Sr, Nd, and Pb isotope geochemistry of MORB. *Chem. Geol.* **62**, 157-176.
- JOHNSON, H.P., KARSTEN, J.L., VINE, F.J., SMITH, G.C. & SCHONHARTING, G. (1982): A low level magnetic survey over a massive sulphide orebody in the Troodos ophiolite complex, Cyprus. *Marine Technol. Soc. J.* **16**, 76.
- KAPPEL, E.S. & FRANKLIN, J.M. (1988): The relationship between geological development of ridge crests and sulfide deposits in the northeast Pacific Ocean. *Econ. Geol.* (in press).
- KOENIG, J.B. (1967): The Salton-Mexicali geothermal province. *California Div. Mines Geol., Mineral Inf. Service* **20**.
- LALOU, C., BRICHET, E., JEHANNO, C. & PEREZ-LECLAIRE, H. (1983): Hydrothermal manganese oxide deposits from the Galapagos mounds, DSDP Leg 70, hole 504B and "Alvin" dives 729 and 721. *Earth Planet. Sci. Lett.* **63**, 63-75.
- LANGMUIR, C.H., BENDER, J. & BATIZA, R. (1986): Petrological and tectonic segmentation of the East Pacific Rise, 5°30'–14°30'N. *Trans. Amer. Geophys. Union* **67**, 422-429.
- LYDON, J.W. & GALLEY, A. (1986): The chemical and mineralogical zonation of Mathiati alteration pipe, Cyprus, and genetic significance. In *Metallogeny of Basic and Ultrabasic Rocks* (M.J. Gallagher, R.A. Ixer, C.R. Neary & H.M. Prichard, eds.). Inst. Mining Metall., London, U.K., 49-68.
- MACDONALD, K.C., SEMPERE, J.C. & FOX, P.J. (1984): East Pacific Rise from Siqueros to Orozco Fracture Zones: Along-strike continuity of axial neovolcanic zone and structure and evolution of overlapping spreading centers. *J. Geophys. Res.* **89**, 6049-6069.
- _____, _____ & _____ (1986): Reply: The debate concerning overlapping spreading centers and mid-ocean ridge processes. *J. Geophys. Res.* **91**, 10501-10511.
- MACDOUGALL, J.D. & LUGMAIR, G.W. (1986): Sr and Nd isotopes in basalts from the East Pacific Rise: significance for mantle heterogeneity. *Earth Planet. Sci. Lett.* **77**, 273-284.
- MALAHOFF, A., EMBLEY, R.W., CRONAN, D.S. & SKIRROW, R. (1983): The geological setting and chemistry of hydrothermal sulfides and associated deposits from the Galapagos Rift at 86°W. *Mar. Mining* **4**, 123-137.
- MCCULLOCH, M.T., GREGORY, R.T., WASSERBURG, G.J. & TAYLOR, H.P., JR. (1981): Sm-Nd, Rb-Sr and ¹⁸O/¹⁶O isotopic systematics in an oceanic crustal section: Evidence from the Samail ophiolite. *J. Geophys. Res.* **86**, 2721-2735.
- MCGREGOR, B.A. & RONA, P.A. (1975): Crest of the Mid-Atlantic Ridge at 26°N. *J. Geophys. Res.* **80**, 3307-3314.
- MORTON, R.L. & FRANKLIN, J.M. (1987): Two-fold classification of Archean volcanic-associated massive sulfide deposits. *Econ. Geol.* **82**, 1057-1063.
- MOTTL, M.J. (1983): Metabasalt, axial hot springs, and the structure of hydrothermal systems at mid-ocean ridges. *Geol. Soc. Amer. Bull.* **94**, 161-180.

- PARKER, R.L. & HEUSTIS, S.P. (1974): The inversion of magnetic anomalies in the presence of topography. *J. Geophys. Res.* **79**, 1587-1593.
- PERFIT, M.R. & FORNARI, D.J. (1983): Geochemical studies of abyssal lavas recovered by DSRV ALVIN from Eastern Galapagos rift, Inca transform, and Ecuador rift, 2. Phase chemistry and crystallization history. *J. Geophys. Res.* **88**, 10530-10550.
- _____, _____, MALAHOFF, A. & EMBLEY, R.W. (1983): Geochemical studies of abyssal lavas recovered by DSRV ALVIN from eastern Galapagos rift, Inca transform and Ecuador rift, 3. Trace element abundances and petrogenesis. *J. Geophys. Res.* **88**, 10551-10572.
- PHILLIPS, J.D., WOODSIDE, J. & BOWIN, C.O. (1969): Magnetic and gravity anomalies in the Central Red Sea. In *Hot Brines and Recent Heavy Metal Deposits in the Red Sea* (E.T. Degens & D.A. Ross eds.), 98-113. Springer-Verlag, New York.
- PLYUSNINA, I.I. (1984): A special state of low-temperature silica in the transition, gel > cristobalite > quartz. *Dokl. Akad. Nauk SSSR* **279**, 1474-1478. (Eng. transl. 189-193).
- RENARD, V., HÉKINIAN, R., FRANCHETEAU, J., BALLARD, R.D. & BÄCKER, H. (1985): Submersible observations at the axis of the ultra fast-spreading East Pacific Rise (17°30' to 21°30'S). *Earth Planet. Sci. Lett.* **75**, 339-353.
- RICHARDS, H.G., CANN, J.R. & JENSENSIUS, J. (1988): Mineralogical and metasomatic zonation of the alteration zone of Cyprus sulfide deposits. *Econ. Geol.* (in press).
- RISE PROJECT GROUP (1980): East Pacific Rise: hot springs and geophysical experiments. *Science* **207**, 1421-1433.
- ROBERTS, R.G. & REARDON, E.J. (1978): Alteration and ore-forming processes at Mattagami Lake Mine, Quebec. *Can. J. Earth Sci.* **15**, 1-21.
- ROBINSON, P.T., MELSON, W.G., O'HEARN, T. & SCHMINCKE, H.-U. (1983): Volcanic glass compositions of the Troodos ophiolite, Cyprus. *Geology* **11**, 400-404.
- RONA, P. A. (1978): Magnetic signatures of hydrothermal alteration and volcanogenic mineral deposits in oceanic crust. *J. Volcanol. Geothermal Res.* **3**, 219-225.
- _____. (1984): Hydrothermal mineralization at seafloor spreading centers. *Earth Sci. Rev.* **20**, 1-104.
- SCHMINCKE, H.-U., RAUTENSCHLEIN, M., ROBINSON, P.T. & MEHEGER, J.M. (1983): Troodos extrusive sequence of Cyprus: A comparison with oceanic crust. *Geology* **11**, 405-409.
- SEYFRIED, W.E. & JANECKY, D.R. (1985): Heavy metal and sulfur transport during subcritical and supercritical hydrothermal alteration of basalt; influence of fluid pressure and basalt composition and crystallinity. *Geochim. Cosmochim. Acta* **49**, 2545-2560.
- SHIMAZAKI, H. & MACLEAN, W.H. (1976): An experimental study on the partition of zinc and lead between the silicate and sulfide liquids. *Mineral. Deposita* **11**, 125-132.
- SMITH, M.F. (1987): *Geochemical Constraints on Alteration in the Galapagos Fossil Hydrothermal System*. M.Sc. thesis. Univ. of Florida, Gainesville, Florida.
- _____, PERFIT, M.R., JONASSON, I.R. & EMBLEY, R.W. (1986): Geochemical constraints on the development of the Galapagos massive sulfide deposit. *EOS, Trans. Amer. Geophys. Union* **91**, 1185.
- SPOONER, E.T.C., BECKINSOLE, R.D., FYFE, W.S. & SMEWING, J.D. (1974): ¹⁸O-enriched ophiolite metabasic rocks from East Liguria (Italy), Pindos (Greece) and Troodos (Cyprus). *Contr. Mineral. Petrology* **47**, 41-62.
- _____, CHAPMAN, H.J. & SMEWING, J.D. (1977): Strontium isotopic contamination and oxidation during ocean floor hydrothermal metamorphism of the ophiolitic rocks of the Troodos Massif, Cyprus. *Geochim. Cosmochim. Acta* **41**, 873-890.
- STAKES, D.S. & O'NEILL, J.R. (1982): Mineralogy and stable isotope geochemistry of hydrothermally altered oceanic rocks. *Earth Planet. Sci. Lett.* **57**, 285-304.
- _____, TAYLOR, H.P. & FISHER, R.L. (1983): Oxygen-isotope and geochemical characterization of hydrothermal alteration in ophiolite complexes and modern oceanic crust. In *Ophiolites and Oceanic Lithosphere* (I. G. Goss, S. J. Leppard & A. W. Shelton, eds.). Geol. Soc. London, Blackwell Sci. Publ., Oxford, 199-214.
- STUDT, F.E. (1959): Magnetic survey of the Wairakei hydrothermal field. *New Zealand J. Geol. Geophys.* **2**, 746-752.
- VIDAL, PH. & CLAUER, N. (1981): Pb and Sr isotopic systematics of some basalts and sulphides from the East Pacific Rise at 21°N (project RITA). *Earth Planet. Sci. Lett.* **55**, 237-246.
- VOGT, P.R. & DE BOER, J. (1976): Morphology, magnetic anomalies and basalt magnetization at the ends of the Galapagos high-amplitude zone. *Earth Planet. Sci. Lett.* **33**, 145-163.
- WHITE, W.M., HOFFMAN, A.W. & PUCHELT, H. (1987): Isotope geochemistry of Pacific mid-ocean ridge basalt. *J. Geophys. Res.* **92**, 4881-4893.

Received August 8, 1987; revised manuscript accepted May 27, 1988.